RE-552

ADVANTAGES OF RESIDUAL STRESSES IN DYNAMICALLY RIVETED JOINTS

February 1978

Grumman Research Department Report RE-552

ADVANTAGES OF RESIDUAL STRESSES IN DYNAMICALLY RIVETED JOINTS.

by Research rept.

Basil P. Leftheris

Fluid Dynamics

Feb[redacted]78

80p

Approved by: Richard A. Scheuing
Richard A. Scheuing
Director of Research

406 165

ABSTRACT

This report presents an analytical method for calculating residual stresses in joints riveted dynamically, results of the Moire experimental method for measuring the residual strain distribution around a rivet hole, and describes an experimental method for measuring the radial velocity of an expanding rivet. The advantages of compressive residual stresses in dynamically riveted joints are demonstrated through constant amplitude fatigue testing.

The particular cases in which residual stresses were investigated include aluminum 7075-T6 and 2024-T3 sheet with $\frac{1}{4}$ in. diameter holes, riveted with A-286 rivets installed with the Stress Wave Riveter. Stress wave riveting expands the rivet radially under high acceleration to achieve favorable stress distributions. Analytical predictions of these stress distributions are compared with experimental results obtained using the Moire photoelastic method. To demonstrate the benefits of compressive residual stresses in riveted joints, fatigue specimens made of 2024-T81 aluminum were used. The specimens were tested at constant amplitude load cycling. In the first series of tests, the fatigue life of specimens with residual stresses was approximately ten times higher than the fatigue life of specimens with open holes. In the second series, precracked specimens with a 0.05 in. crack in each hole were riveted with the Stress Wave Riveter. The cracks were oriented so that the fatigue loading was normal to the crack path. The fatigue life of these specimens was also approximately ten times higher than the fatigue life of those specimens with precracked holes without rivets.

TABLE OF CONTENTS

LIST OF ILLUSTRATIONS

LIST OF SYMBOLS

u	particle velocity
r	radial displacement
t	time
E	Young's modulus
s	stress deviation
e	mean normal strain
k	bulk modulus
K	yield stress in pure shear
m	constant (rate of acceleration)
a	radius of hole
b	radius where residual stresses become zero
R	radius of elastic plastic interface

Greek Letters

ρ	density
σ	stress
ϵ	strain
μ	Poisson's ratio

Subscripts

r	radial
θ	circumferencial
z	axial
o	initial conditions
y	yield conditions

Superscripts

P	plastic

1. INTRODUCTION

Fatigue life of structures is usually determined by the growth of cracks originating at points of local stress concentration. The holes provided for fasteners in riveted joints are known to be the most probable locations for crack initiation due to a) high frequency of defects in the hole machined surface and b) high concentration of in-service tensile stresses near the hole surface. Substantial and significant benefits in design life and structural weight can be achieved by the use of special techniques to reduce the levels of maximum tensile stress near a hole by introducing residual compressive stresses that prevent or inhibit the growth of cracks under cyclic loading.

It is known that plastically deforming (i.e. cold-working) the hole material induces compressive residual stresses. Dietrich and Potter (Ref. 1) used X-rays to show the existence of residual compressive stresses that resulted from the use of a mandrel. Chang (Ref. 2) showed that such residual stresses do inhibit crack growth and improve fatigue life in riveted joints. This report discusses the prediction and experimental verification of the residual stress distributions that are produced by dynamic installation of rivets.

An important distinction must be made between the following methods of fatigue-resistant fastening:

a) Precision fasteners, or threaded pins, driven into undersized holes (i.e., Taper Loks, High Tigues, etc.)

b) Fasteners that take advantage of residual stresses induced in the hole through burnishing, peening, or forming using a mandrel or a hard steel ball. The fastener is of secondary importance in these methods.

c) Rivet-type methods which utilize a rivet that is usually subjected to higher loads than those necessary to fill the hole, thereby producing residual compressive stresses in the surrounding metal.

Precision fasteners (a) require precision holes (typical tolerances of ± 0.001 in.), and after they are installed there is little unloading that could allow the material that expanded plastically to relax with significant compressive residual stresses. Fastener, hole preparation and quality control costs are usually quite high with these methods. Residual stresses are produced in (b), where a section of the hole is put in a plastic state so that the surrounding elastic material squeezes that section as it does in the "autofrettage" treatment of thick-wall cylinders (Ref. 3). This class of processes is labor-intensive, and has not yet been successfully automated.

This report is also concerned with the computation of residual stresses and strains by dynamic methods of the type described in (c), which offers very inexpensive fastening. Of the types of riveting processes included in (c) we shall consider only dynamic riveting where the rivet expands with sizeable velocity and large radial accelerations. One such process is implemented by the Stress Wave Riveter (Ref. 4).

There are various methods available for calculating residual stresses (Refs. 5, 6). Most of them are implemented by computer programs using finite element schemes. The difficulty with these programs lies in their inability to do numerical examples with various cases without extensive involvement of the user toward understanding the program itself. In this work explicit equations are used that provide a well-defined series of equations

that can be solved on a programmable desk calculator. The user can readily understand the cause and effect relationship in every new case without the commitment inherent in large computer programs.

2. DERIVATION OF EQUATIONS

PROBLEM DESCRIPTION

In riveting with the Stress Wave tool, a rivet is placed in a hole with the bucking bar on one side and the Stress Wave tool on the other (see Fig. 1a). At first the stress wave overcomes the elastic limit of the rivet material and sets it in plastic flow (Ref. 4). Subsequently, as the massive head of the Stress Wave tool (see Fig. 1b) moves axially against the rivet, the rivet expands radially out toward the surface of the hole. The analysis in this report is concerned with the stress and strain distribution in the material around the hole, from the time ($t = 0$) when the rivet impacts the hole surface to the time ($t = t_3$) when the dynamic process of riveting terminates. In formulating the problem of stress distribution we have hoop stress (σ_θ), hoop strain (ϵ_θ), radial stress (σ_r) and radial strain (ϵ_r); also, (r_o), (the radial position prior to the riveting disturbance) and the time, (t). The following two boundary conditions are used: a) the velocity history at $r_o = a$ (see Fig. 1c) and b) the condition of zero stress and strain at some radius far away from the hole $r_o = b$.

The velocity history at $r_o = a$ is found experimentally (see Fig. 2). It has three parts: a) linear loading from $t = 0$ to $t = t_o$, b) constant velocity from $t = t_o$ to $t = t_2$, and c) unloading from $t = t_2$ to $t = t_3$. Figure 2 shows the entire riveting sequence by plotting strain vs. time. Reference 4 describes the process in complete detail.

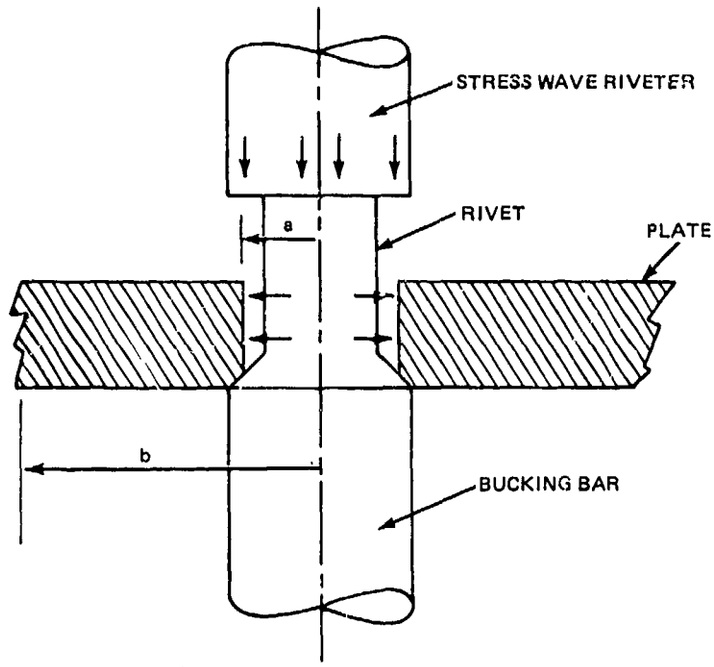

A) STRESS WAVE TOOL SETUP

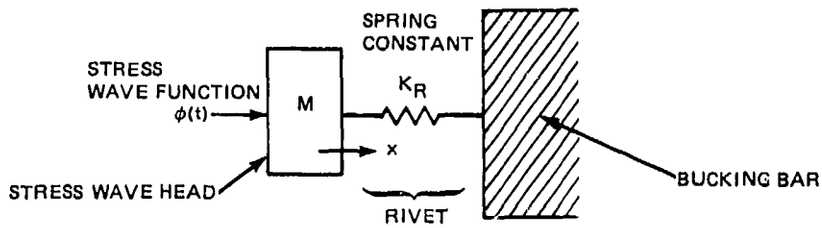

B) EQUIVALENT SCHEMATIC OF STRESS WAVE RIVETING

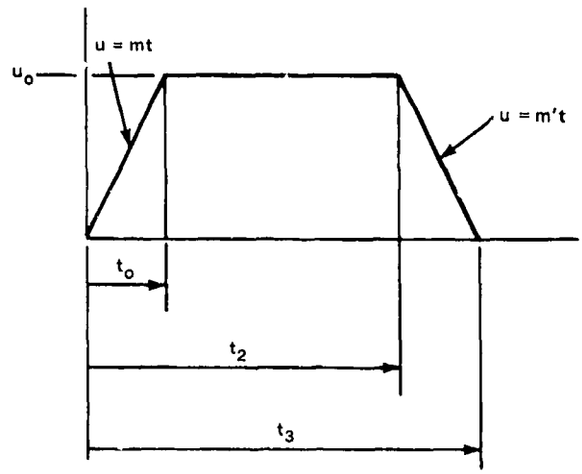

C) VELOCITY HISTORY AT $r_o = a +$

Fig. 1 Concept of Stress Wave Riveting

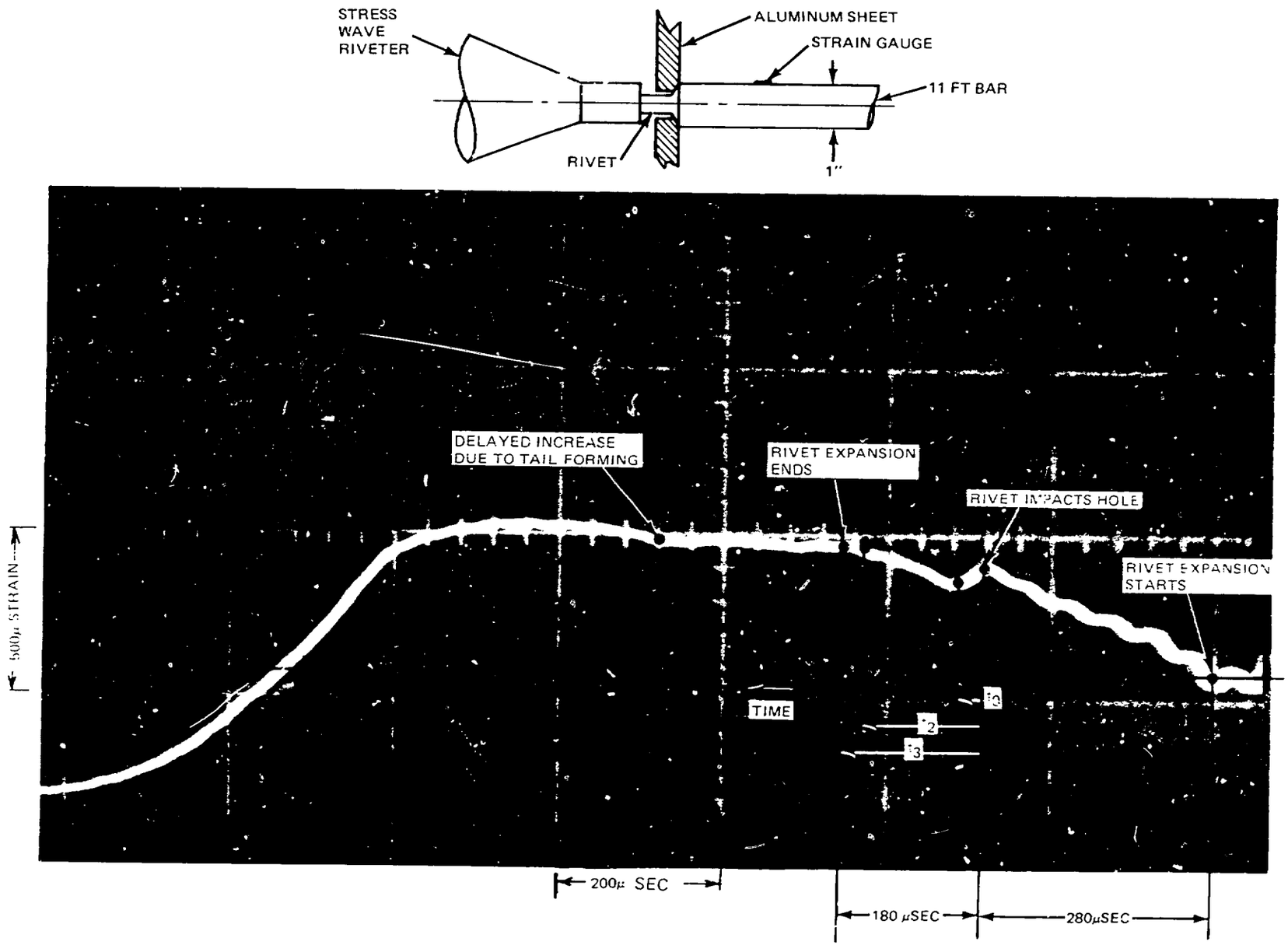

Fig. 2 Strain Gauge Record of 1/4 in. A-286 Rivet

GENERAL RELATIONS

The relations used in elastoplastic problems of cylinders under internal pressure are suitable for our application with rivets. In polar coordinates, assuming axisymmetric conditions, these relations are as follows (Ref. 7).

Equilibrium Equation in Radial Direction

$$\rho \frac{\partial u}{\partial t} + \frac{\partial \sigma_r}{\partial r_o} + \frac{\sigma_r - \sigma_\theta}{r_o} = 0 \tag{1}$$

Compatibility Equation

$$\frac{\partial \epsilon_\theta}{\partial r_o} + \frac{\epsilon_\theta - \epsilon_r}{r_o} = 0 \tag{2}$$

Incompressibility Equation

$$\epsilon_r + \epsilon_\theta + \epsilon_z = 0 \tag{3}$$

Strain Displacement Relations (See Appendix A)

$$\epsilon_\theta = r/r_o \tag{4}$$

$$\epsilon_r = \frac{\partial r}{\partial r_o} \tag{5}$$

Stress-Strain Relations

$$\epsilon_r = \frac{1}{E}[\sigma_r - \mu(\sigma_\theta + \sigma_z)] + \epsilon_r^p$$

$$\epsilon_\theta = \frac{1}{E}[\sigma_\theta - \mu(\sigma_r + \sigma_z)] + \epsilon_\theta^p \tag{6}$$

$$\epsilon_z = \frac{1}{E}[\sigma_z - \mu(\sigma_r + \sigma_\theta)] - (\epsilon_\theta^p + \epsilon_r^p)$$

For cases of plane stress $\sigma_z = 0$ and for plane strain $\epsilon_z = 0$. In both cases the shear stresses and strains are zero. The plane strain condition will be used in this analysis.

In our analysis we find it convenient to use the mean normal stress defined as (Ref. 5)

$$S = \frac{1}{3}(\sigma_r + \sigma_\theta + \sigma_z)$$

where σ_r, σ_θ, and σ_z are the principle stresses.

The principle components of the stress deviator tensor are as follows

$$S_r = \sigma_r - S,\ S_\theta = \sigma_\theta - S,\ S_z = \sigma_z - S \tag{7}$$

In the analysis we use the deformation theory (Ref. 7, p. 120) (in contrast to incremental or flow theories) in which the plastic strains are functions of the current state of stress and are independent of the history of loading. We are permitted to use the deformation theory because of the axial symmetry and radial loading of the problems encountered in riveting and because we consider separately the loading and unloading history of the problem.

The mean normal strain is given by

$$e = \frac{1}{3}(\epsilon_r + \epsilon_\theta + \epsilon_z) \tag{8}$$

such that Hooke's law can be expressed by: (see Appendix A)

$$S = 3k \cdot e \quad , \text{ where k is the bulk modulus} = \frac{E}{3(1-2\mu)} \tag{9}$$

The principal strain components are given by

$$e_r = \epsilon_r - e,\ e_\theta = \epsilon_\theta - e \text{ and } e_z = \epsilon_z - e$$

Under the incompressibility assumption, however, $e = 0$ thus

$$e_r = \epsilon_r \ , \ e_\theta = \epsilon_\theta \text{ and } e_z = \epsilon_z$$

The following expressions of the generalized Hooke's law can be used

$$\sigma_r = \frac{9\mu}{(1+\mu)} k \cdot e + \frac{E}{(1+\mu)} \epsilon_r \ , \ \sigma_z = \frac{9\mu}{(1+\mu)} k \cdot e + \frac{E}{(1+\mu)} \epsilon_z$$

and

$$\sigma_\theta = \frac{9\mu}{(1+\mu)} k \cdot e + \frac{E}{(1+\mu)} \epsilon_\theta$$

We observe that incompressibility does not permit us to solve for S in the equation $3k \cdot e = S$, since, when $e \to o$, we have $k \to \infty$. From Hooke's law, however, we know that $\sigma_r + \sigma_\theta + \sigma_z = 9k \cdot e$, which leads us to conclude that $S_r + S_\theta + S_z = 0$. Furthermore, from the definition of S_r, S_θ and S_z and Hooke's law we find

$$S_r = E' \epsilon_r$$

$$S_\theta = E' \epsilon_\theta \qquad (10)$$

and $$S_z = E' \epsilon_z$$

where

$$E' = \frac{E}{1+\mu} \quad \text{(see Appendix A).}$$

Considering the case of plane strain where $\epsilon_z = 0$ and $S_z = 0$ at all times, we have

$$\epsilon_r + \epsilon_\theta = 0$$

and $$S_r + S_\theta = 0 \qquad (10a)$$

CRITERIA FOR YIELDING

In order to extend our analysis to problems of riveting with plastic deformations we must set up criteria for yielding. It is generally accepted that hydrostatic pressure does not produce appreciable plastic deformation. Instead, it is usually assumed that plastic deformation depends only on the stress deviation.

Using the well known Von Mises criterion (Ref. 7) for yielding, we have

$$\frac{1}{\sqrt{6}} \left[(S_r - S_\theta)^2 + (S_\theta - S_z)^2 + (S_z - S_r)^2\right]^{\frac{1}{2}} = K \qquad (11)$$

where K is the yield stress in pure shear. It can be shown (Ref. 5), that $K = \sigma_o/\sqrt{3}$ where σ_o is the yield stress in the uniaxial tension loading.

Thus, with $S_z = 0$

$$S_r^2 + S_r S_\theta + S_\theta^2 = K^2 \qquad (12)$$

APPLICATIONS TO DYNAMIC RIVETING

Combining Eqs. (1) and (3) we obtain a system of linear first order partial differential equations that describe the initial (elastic) motion of the rivet.

$$\rho \frac{\partial u}{\partial t} + \frac{\partial \sigma_r}{\partial r_o} + \frac{\sigma_r - \sigma_\theta}{r_o} = 0$$

where $u = \frac{\partial r}{\partial t}$

and $$\frac{\partial r}{\partial r_o} + \frac{r}{r_o} = 0$$

This equation is obtained by substituting the strain conditions into the incompressibility conditions. Substituting for σ_r and σ_θ from Eq. (7), and differentiating the second equation with respect to time we obtain

$$\rho \frac{\partial u}{\partial t} + \frac{\partial S}{\partial r_o} = - \frac{\partial S_r}{\partial r_o} - \frac{(S_r - S_\theta)}{r_o}$$

and (13)

$$\frac{\partial u}{\partial r_o} + \frac{u}{r_o} = 0$$

The above two partial differential equations can be reduced to one partial differential equation, with one dependent variable S and two independent variables r_o and t, by employing Eq. (3) to obtain ϵ_θ and Eq. (10) to obtain S_r and S_θ in terms of S. The velocity function u(t) at $r_o = a$, and the fact that $S = 0$ at all times at $r_o = b$ ($b >> a$), are the two boundary conditions used in the solution. Details are given in Appendix B.

The elastic solution for the stresses and strains is as follows:

$$\sigma_r = \rho m a \ell n(\frac{b}{r_o}) - \frac{E' m t^2 a}{2 r_o^2}$$

$$\sigma_\theta = \rho m a \ell n(\frac{b}{r_o}) + \frac{E' m t^2 a}{2 r_o^2} \qquad (14)$$

$$\epsilon_r = - \frac{m t^2 a}{2 r_o^2}$$

and

$$\epsilon_\theta = \frac{m t^2 a}{2 r_o^2}$$

RELATIONS UNDER PLASTIC DEFORMATION

Plastic deformation begins at $r_o = a$, whenever the radial pressure increases to the point that $S_r = -K$ and $S_\theta = +K$ such that

Von Mises' criterion for yielding applies; that is, $S_r^2 + S_r S_\theta + S_\theta^2 = K^2$. Substituting $S_r = -K$ at $r_o = a$ in the first Eq. of (14) we can find the time t_p that yielding will commence.

$$t_p = \left\{ \frac{2Ka(1+\mu)}{Em} \right\}^{\frac{1}{2}} \tag{15}$$

The stress and strain relations in the plastic region are derived as in the elastic case. Since the incompressibility relation applies to both elastic and plastic cases, the velocity relationship is the same, that is,

$$u = \frac{mat}{r_o}$$

Considering materials that are perfectly plastic, we have

$$\sigma_r = S-K, \quad \sigma_\theta = S+K \text{ and } \sigma_r - \sigma_\theta = 2K$$

Substituting in Eq. (1) we obtain

$$\frac{\rho ma}{r_o} + \frac{\partial S}{\partial r_o} - \frac{2K}{r_o} = 0 \tag{16}$$

Integrating we obtain

$$S = (2K - \rho ma) \ln r_o + f(t)$$

At the elastic-plastic interface ($r_o = R$) both the plastic and elastic solutions hold.

Hence,

$$\sigma_r = S - K = (2K - \rho ma) \ln R + f(t) - K$$

$$= \rho ma \ln \left(\frac{b}{R}\right) - \frac{E' mt^2 a}{2R^2} ,$$

where, $R = \sqrt{\frac{maEt^2}{2K}}$, is the radius of the elastic plastic interface

from which we find,

$$f(t) = K + \rho ma \ell n \left(\frac{b}{R}\right) - \frac{E' mt^2 a}{2R^2} - (2K - \rho ma) \ell n R \qquad (17)$$

Thus, the stresses in the region $a \leq r_o \leq R$ are given by

$$\left.\begin{aligned} \sigma_r^p &= (\rho ma - 2K) \ell n \frac{R}{r_o} + \rho ma \ell n \left(\frac{b}{R}\right) - \frac{E' mt^2 a}{2R^2} \\ \sigma_\theta^p &= (\rho ma - 2K) \ell n \frac{R}{r_o} + 2K + \rho ma \ell n \left(\frac{b}{R}\right) - \frac{E' mta^2}{2R^2} \end{aligned}\right\} \qquad (18)$$

The stresses in the region $R \leq r_o \leq b$ are given by Eq. (14).

REGION OF CONSTANT VELOCITY

In the two previous sub-sections, the elastic and plastic solutions of the stress and strain distributions were found for the loading phase where the velocity of the hole surface was a linear function of time (i.e., $u = mt$). In this section, the solution is extended to the region where the velocity at $r_o = a$ remains constant (i.e., $u = u_o$).

The solutions are derived in Appendix C. The elastic solutions (i.e., $r_o \geq R_1$) are given by

$$\left.\begin{aligned} r &= \rho ma \ell n \left(\frac{b}{r_o}\right) - \frac{E' mat_o}{r_o^2} \left(t - \frac{t_o}{2}\right) \\ \sigma_\theta &= \rho ma \ell n \left(\frac{b}{r_o}\right) + \frac{E' mat_o}{r_o^2} \left(t - \frac{t_o}{2}\right) \\ \epsilon_r &= - \frac{mat_o}{r_o^2} \left(t - \frac{t_o}{2}\right) \end{aligned}\right\} \qquad (19)$$

and

$$\epsilon_\theta = \frac{mat_o}{r_o^2}\left(t - \frac{t_o}{2}\right) \qquad (19)\ (\text{cont})$$

The plastic solution, (i.e., $a \le r_o \le R_1$) are given by

$$\left.\begin{aligned}\sigma_r^p &= \rho ma\ell n\left(\frac{b}{R_1}\right) - \frac{E' mat_o}{R_1^2}\left(t - \frac{t_o}{2}\right) + 2K\,\ell n\frac{r_o}{R_1}\\ \sigma_\theta^p &= \rho\beta ma\ell n\left(\frac{b}{R_1}\right) - \frac{E' mat_o}{R_1^2}\left(t - \frac{t_o}{2}\right) + 2K\,\ell n\frac{r_o}{R_1} + 2K\end{aligned}\right\} \qquad (20)$$

where R_1 is the radius of the elastic-plastic interface.

SOLUTIONS DURING UNLOADING

The final solutions for the distributions of stresses and strains around the hole are found by considering the unloading phase. During this phase the velocity of the hole surface undergoes a linear deceleration (i.e., $u = m' t$) from u_o to zero. The derivation of the equation is similar to the loading and constant velocity cases discussed earlier.

In the derivation of the equations of stress and strain distribution for the constant loading phase we have used the velocity stress, and strain conditions at $t = t_o$ and $r_o = a$ as initial conditions; similarly, we use the conditions at $t = t_2$, and $r_o = a$ as initial conditions for the unloading phase. The stress and strain distributions at the end of the unloading phase, $u = 0$, are the conditions that will be used in the next section to derive the residual stresses and strains.

For the elastic region where $r_o \geq R'$ we have: (see Appendix D)

$$\left.\begin{aligned} \sigma_r &= \rho m' a \ell n \left(\frac{b}{r_o}\right) - \frac{E' a}{r_o^2} F(t) \\ \sigma_\theta &= \rho m' a \ell n \left(\frac{b}{r_o}\right) + \frac{E' a}{r_o^2} F(t) \end{aligned}\right\} \quad (21a)$$

$$\left.\begin{aligned} \epsilon_r &= -\frac{a}{r_o^2} F(t) \\ \epsilon_\theta &= \frac{a}{r_o^2} F(t) \end{aligned}\right\} \quad (21b)$$

where

$$F(t) = mt_o t' + \frac{m'(t')^2}{2} + mt_o t_2 - \frac{mt_o^2}{2}, \text{ where } t' = t - t_2 \quad (22)$$

For the plastic region of $a \leq r_o \leq R'$ the equations for the stress distribution are

$$\left.\begin{aligned} \sigma_r^p &= (2K - \rho m' a) \ell n\left(\frac{r_o}{R'}\right) + \rho m' a \ell n \left(\frac{b}{R'}\right) - \frac{E' a F(t)}{(R')^2} \\ \sigma_\theta^p &= (2K - \rho m' a) \ell n\left(\frac{r_o}{R'}\right) + \rho m' a \ell n \left(\frac{b}{R'}\right) - \frac{E' a F(t)}{(R')^2} + 2K \end{aligned}\right\} \quad (23a)$$

The equations of strain distribution are given by

$$\left.\begin{aligned} \epsilon_r &= -\frac{a}{r_o^2} F(t) \\ \epsilon_\theta &= \frac{a}{r_o^2} F(t) \end{aligned}\right\} \quad (23b)$$

3. RESIDUAL STRESSES: DERIVATION OF EQUATIONS

DERIVATION OF EQUATION FOR INTERFACE PRESSURE

Although the velocity at the end of the unloading phase is zero, the final state of equilibrium between the rivet and surrounding material does not occur until the materials relax under the existing internal forces. The degree of relaxation varies according to the growth of the elastic-plastic radius during loading and also the Young's modulus of each material.

Let us assume that in the final state of equilibrium, the interface pressure between the rivet and the hole is P. The change of the radial stress at $r_o = a$ (the rivet-hole interface) is $\Delta P = (\sigma_r^p - P)$, where σ_r^p is given by Eq. (23) evaluated at $r_o = a$ and $t = t_3$ (the end of the velocity cycle). The radial displacement at $r_o = a$, due to the unloading of the material surrounding the rivet, assuming incompressibility, is given by (Ref. 8, p. 110)

$$\Delta d_1 = - (\sigma_r^P - P) \frac{(1+\mu_1) b^2 a}{E_1} \qquad (24)$$

where the subscript 1 is in reference to the material surrounding the rivet, and $b \gg a$.

At the end of the velocity cycle, when the velocity is zero, the rivet is in dynamic equilibrium. The stress deviators that caused the plastic deformation in the rivet during the velocity cycle are zero. As a result of these conditions the rivet is still under an axial stress from the Stress Wave Tool that is equal to the radial stress σ_r^p, the load from the surrounding material: or, in other words, the rivet before unloading, is under hydrostatic pressure σ_r^P.

It can be shown that if the rivet is considered separately as a free body under hydrostatic pressure σ_r^p, the rivet does not change in size when σ_r^p is removed. Therefore, when the load due to the Stress Wave Riveter is removed, the radial change in the rivet is due to the unloading of the surrounding material, or to the external pressure P. Thus the radial displacement of the rivet during unloading is given by (Ref. 3, p. 322)

$$\Delta d_2 = -\frac{P}{E_2}(1-\mu_2) \tag{25}$$

where the subscript 2 is in reference to the rivet material.

The condition of compatibility at the rivet-hole interface, after complete unloading, is

$$\Delta d_1 = \Delta d_2 \qquad \text{or}$$

$$-(\sigma_r^p - P) = \frac{(1+\mu_1)b^2 a}{E_1(b^2-a^2)} = -\frac{P(1-\mu_2)a}{E_2}$$

Hence,

$$P = \frac{\left(\frac{1+\mu_1}{1-\mu_2}\right)\left(\frac{E_2}{E_1}\right)(\sigma_r^p)_{r_o=a}}{1+\left(\frac{1+\mu_1}{1-\mu_2}\right)\left(\frac{E_2}{E_1}\right)} \tag{26}$$

The stresses at the end of the unloading period are given by

$$\sigma_r = \sigma_r^p + \Delta\sigma_r \text{ and } \sigma_\theta = \sigma_\theta^p + \Delta\sigma_\theta \tag{27a}$$

where

$$\Delta\sigma_r = \left\{\left(\sigma_r^p\right)_{r_o=a} - P\right\}\frac{a^2}{b^2-a^2}\left(1-\frac{b^2}{r_o^2}\right) \tag{27b}$$

and

$$\Delta\sigma_\theta = \left\{ \left(\sigma_r^p \right)_{r_o = a} - P \right\} \frac{a^2}{b^2 - a^2} \left(1 + \frac{b^2}{r_o^2} \right) \tag{27b}$$

The values of σ_r^p and σ_θ^p are given by Eq. (23) for $t = t_3$. The circumferential strain at the end of phase 3 (i.e. $t = t_3$) is found from Eqs. (23b).

The change in circumferential strain for the unloading phase is given by

$$\Delta\epsilon_\theta = \left\{ P - \left(\sigma_r^p \right)_{r_o = a} \right\} \left(\frac{1+\mu_1}{E_1} \right) \cdot \frac{a^2}{r_o^2}$$

and the change of radial strain is given by

$$\Delta\epsilon_r = - \left\{ P - \left(\sigma_r^p \right)_{r_o = a} \right\} \left(\frac{1+\mu_1}{E_1} \right) \cdot \frac{a^2}{r_o^2}$$

Thus, the final residual strain distributions are given by

$$(\epsilon_\theta)_f = \epsilon_\theta + \Delta\epsilon_\theta \tag{28a}$$

$$(\epsilon_r)_f = \epsilon_r + \Delta\epsilon_r \tag{28b}$$

CONDITIONS OF UNLOADING WITH YIELDING

Prager and Hodge (Ref. 8, p. 111) treat this case, so we need only incorporate their solution. The criterion for yielding is the radial stress change $\left\{ \left(\sigma_r^p \right)_{r_o = a} - P \right\} = \Delta P$, where $\left(\sigma_r^p \right)$ is obtained from Eq. (23a).

When $\Delta P > 2K \left(1 - \frac{a^2}{b^2} \right)$, yielding occurs (Ref. 8, p. 105). The value of ΔP, derived from elastic conditicns of unloading, will provide an upper bound value for the radius of the elastic-plastic interface. This assumption is justified, since the value of R_2 is close to the value of $r_o = a$.

The value of R_2 can be calculated from (Ref. 8, p. 110)

$$2 \ell n \frac{b}{R_2} + \frac{R_2^2}{b^2} - 1 = 2 \ell n \frac{b}{a} - \frac{\Delta P}{2K} .$$

For $b >> R_2$ we can neglect $\left(\frac{R}{b} \right)^2$. Thus, we obtain

$$R_2 = be^{-1/2(1+2 \ell n \frac{b}{a} - \frac{\Delta P}{2K})} \tag{29}$$

If $R_2 > a$ then yielding is occurring during unloading; if $R_2 < a$ then yielding does not occur and Eqs. (27) and (28) may be used.

In the case where $R_2 > a$ we have the following equations:

$$\Delta \sigma_r = \begin{cases} 2K \left(1 - \frac{R_2^2}{b^2} - 2 \ell n \frac{r_o}{R_2}\right) & a \le r_o \le R_2 \quad (30a) \\ -2K \frac{R_2^2}{b^2} \left(1 - \frac{b^2}{r_o^2}\right) & R_2 \le r_o \le b \quad (30b) \end{cases}$$

$$\Delta \sigma_\theta = \begin{cases} -2K \left(1 + \frac{R_2^2}{b_2} + 2 \ n \frac{r_o}{R_2}\right) & a \le r_o \quad R_2 \quad (31a) \\ -2K \frac{R_2^2}{b^2} \left(1 + \frac{b^2}{r_o^2}\right) & R_2 \le r_o \le b \quad (31b) \end{cases}$$

$$\Delta \epsilon_\theta = - \frac{K R_2^2 (1 + \mu)}{E r_o^2} \tag{32a}$$

$$\Delta\epsilon_r = \frac{K R_2^{\,2}(1+\mu)}{E\, r_o^{\,2}} \tag{32b}$$

The final residual stresses are found by combining Eq. (23a) with Eq. (31) and (,

$$\sigma_r = \sigma_r^p + \Delta\sigma_r \quad , \quad \sigma_\theta = \sigma_\theta^p + \Delta\sigma_\theta \tag{33a}$$

The final residual strains are found by combining Eqs. (23b) and (32)

$$(\epsilon_r)_f = \epsilon_r + \Delta\epsilon_r, \quad (\epsilon_\theta)_f = \epsilon_\theta + \Delta\epsilon_\theta \tag{33b}$$

The residual circumferential strain is found by combining Eqs. (21) and (32). The following flow charts show the sequence of computations for calculating the residual stresses and strains.

FLOW CHARTS FOR CALCULATIONS OF RESIDUAL STRESSES AND STRAINS

a) Stresses and strains at the end of the loading phase

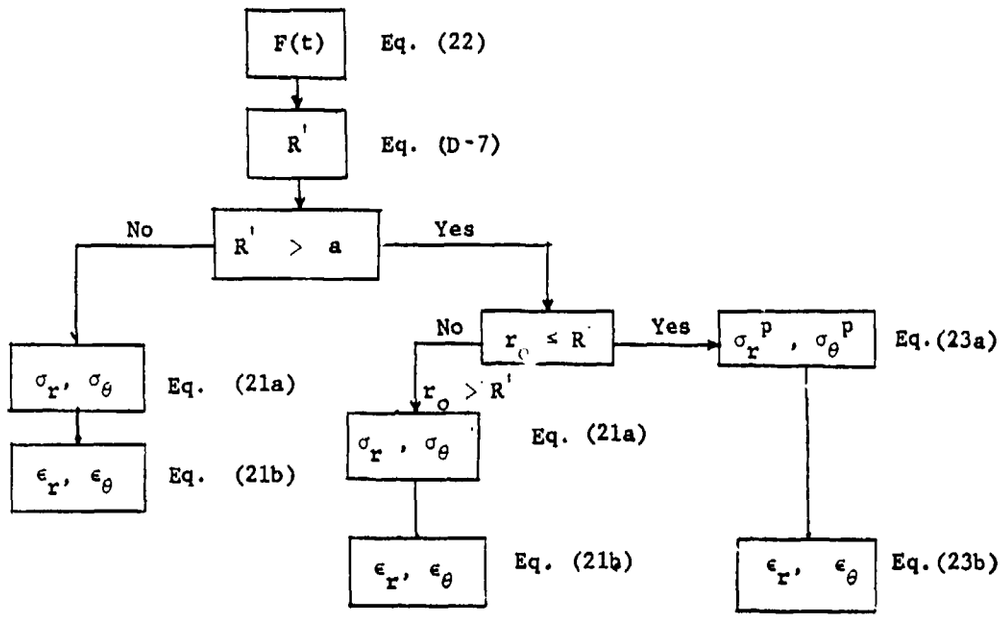

b) Residual stresses and strains at the end of the unloading phase

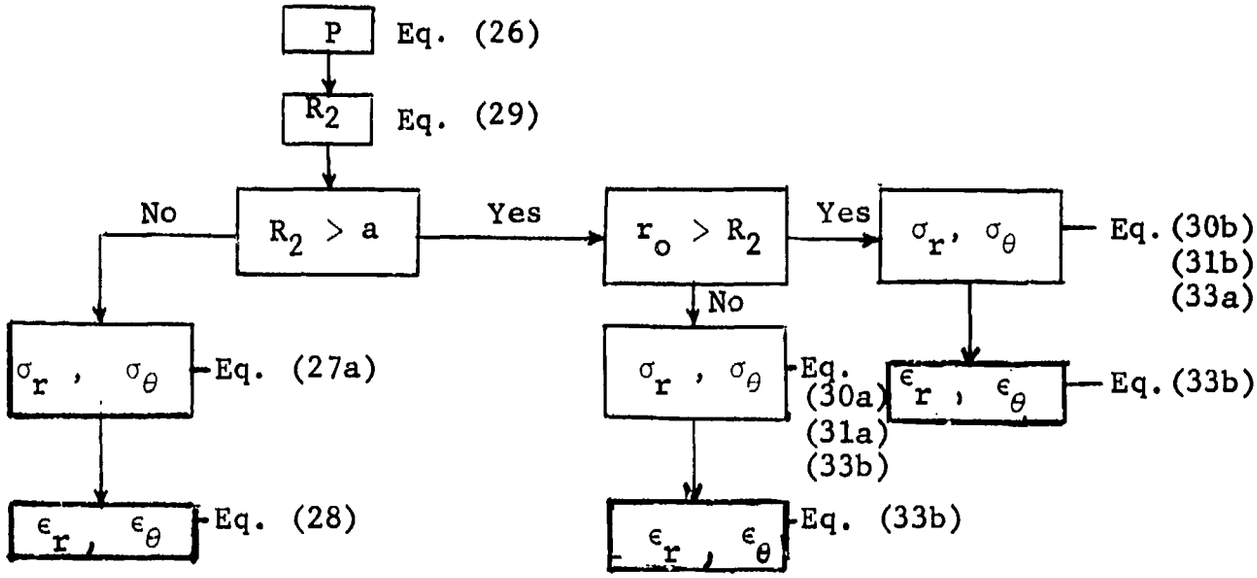

CONDITIONS FOR COMPLETE UNLOADING OF THE HOLE

The equations derived in the previous sections can also be used for the case where the rivet is removed after the normal rivet installation. Such cases are represented by selecting the elastic modulus for the rivet $E_2 = 0$.

The stress and strain distributions for complete unloading by removal of the rivet (i.e., radial stress at the hole surface is zero) are different from the distributions with the rivet in place. The differences and their significance are discussed in Section 5.

Axial stresses are calculated from equations derived in Appendix E. Axial stresses are of special interest in the cases where the rivet is removed and the radial stress at $r_o = a$ is zero; then, the value of the residual hoop stress may be higher than σ_y. This does not mean, however, that we have violated any assumptions since we must also consider the axial stress distributions.

COMPUTATIONS

The four important parameters in our calculations are:

a) Residual radial stress

b) Residual hoop stress

c) Residual hoop strain

c) Residual radial strain.

The following cases can be computed with data already in the program.

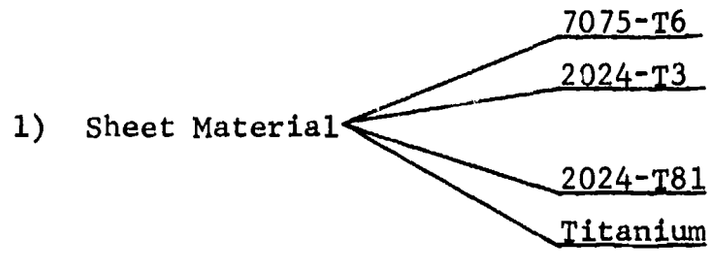

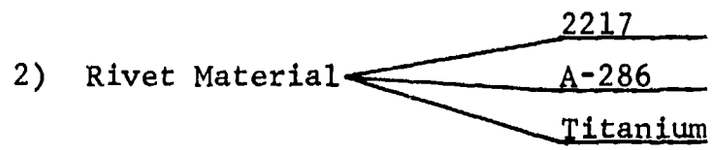

The programs will print out and plot the radial distance versus the residual stresses and strains; then by setting $E_2 = 0$ the residual stresses and strains for complete unloading can be found. The input necessary for the running of the program is the time history of the velocity at the hole surface discussed in Section 4 under Experimental Velocity Measurements.

4. EXPERIMENTAL WORK

INTRODUCTION

There are three separate types of experimental work that have been carried out in this program. The first consists of measuring the force rate ($\frac{lb}{sec}$) in an instrumented 11 foot long steel bar (Ref. 4). This technique is equivalent to the Hopkinson's bar used in earlier work with stress waves (Ref. 9). The second type of experimental work consists of measuring the residual strain photoelastically using the Moire' method.* The results from these tests are compared with the theoretical results discussed earlier. In the third type of experiment, fatigue specimens with precracked holes, riveted with the Stress Wave Riveter, were tested (with precracked unriveted controls) to show the effects of residual stresses in improving the fatigue life of rivet joints.

EXPERIMENTAL VELOCITY MEASUREMENTS

The time intervals t_o, t_2, and t_3 were determined experimentally by instrumented bar measurements. A rivet was placed between the Stress Wave Riveter and the 11 foot bucking bar instrumented with strain gauges (see Fig. 2). As the rivet deforms, the bar records the time history through the strain gauges as the stress wave travels along the bar. The following explanation of the features of the measurements shown in Fig. 2 is based on our present understanding of the forming process.

---

* Grumman Report MMT -379, "Moire' Fringe Analysis of the Strain Fields Surrounding a Stress Wave Driven Rivet," Engineering Test Operations, November 1977.

Initially, the radius of the rivet expands freely inside the hole. Since the cross-sectional area increases during deformation, the force transmitted to the bar increases with time because the plastic modulus is roughly constant. When the rivet impacts the hole surface, there is a momentary drop in force rate due to wave reflection in the rivet. In the particular case shown in Fig. 2 (A-286 rivet in aluminum) the rivet impact shows as a drop in force rate. In this case, the acoustic impedance of the rivet in the plastic state is smaller than the acoustic impedance of the aluminum. As soon as the aluminum becomes plastic, however, the rate at which the force increases is restored. (Aluminum or titanium rivets may show different behaviors.)

The results also show that the rate of force increase with time is approximately constant, which indicates a constant rate of increase in rivet cross-section if the plastic modulus is constant. When the rivet is formed there is no further increase in force, because there is no further increase in area, even though the axial stroke continues. Only when the force associated with forming the tail of the rivet is transmitted through to the bar is there a slight increase in the indicated force.

The time measurements from the typical case of Fig. 2 are used to find the velocity history at the hole surface (r = a). From previous work (Ref. 4) it is known that the acceleration during the loading and deceleration during the unloading phase can be approximated by a linear function of time. The slope of the function is found experimentally by measuring the times of acceleration (or deceleration) and the maximum velocity. The maximum radial velocity is found from the following equation:

$$u_r = u_p \cdot \frac{\alpha_m}{K_r}$$

where

α_m force rate measured at the 11 foot bar

K_r spring constant of the rivet during plastic deformation. $1.18 \times 10^5 \frac{lb}{in.}$

and

u_p Poisson's ratio during plastic flow = $\frac{1}{2}$.

From Figure 2, change of strain during $t = (t_2 - t_o)$ is $\Delta\epsilon = 100 \times 10^{-6} \frac{1}{sec}$, and $\Delta t = 120 \times 10^{-6}$ sec. Thus, $\alpha_m = \frac{\Delta\epsilon}{\Delta t} \cdot E \cdot \frac{\pi}{4} = 19.63 \times 10^6$ and $u_r = 83.2 \frac{in.}{sec}$.

Since during plastic flow of the rivet, the velocity u_r remains essentially constant (Ref. 4) an alternate method to calculate the velocity is to measure the final expansion of the rivet radius so that

$$u_r = \frac{\Delta R}{\Delta t}$$

For the case considered in Fig. 2, $\Delta R = 0.0095$ in.

Hence,

$$u_r = 80 \frac{in.}{sec}$$

The two values, obtained independently, agree well. The value of u_r is the input into the computer program, corresponding to the radial expansion that determines the residual stresses and strains.

EXPERIMENTAL MEASUREMENTS OF RESIDUAL STRAINS

Residual strain can be measured only through nondestructive methods. The measurements used in this work were made by the Moire' technique. To facilitate the proper use of the Moire' method, the riveted plate with the appropriate grid coating was protected during riveting in either side by a $\frac{1}{8}$ in. plate that was removed after riveting, leaving the shank of the rivet inside the coated plate where the residual strain measurements are made (see Fig. 3). After the rivet was installed dynamically with the Stress Wave Riveter head and tail of the rivet were carefully machined off in a lathe until the protective plates dropped off, leaving the center plate with the rivet chank in place. The plate was then used in the laboratory to measure the residual strains. Having obtained the residual strains, the rivet was carefully drilled out without touching the hole surface. The residual strain was measured again (see footnote pg. 25).

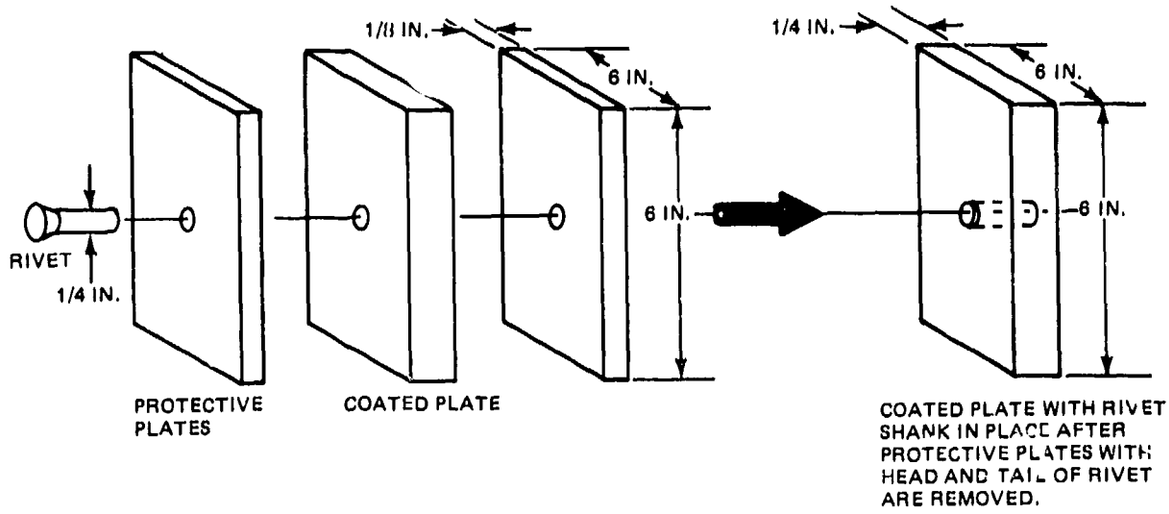

Fig. 3 Specially Designed Specimen for Measuring Residual Strain Using Moire' Technique

We obtained measurements first with the rivet in place and second with the rivet removed which represented complete unloading of the hole. The difference of residual strains in these two cases is substantial, especially near the hole surface. The hole diameter, after the rivet installation, was measured with a magnifying lens. By comparing the hole size with the initial diameter, we could find the hole radial expansion, or amount of interference. Two materials were used for testing; 7075-T6 and 2024-T3. The specimens were 6 x 6 x $\frac{3}{16}$ in. and the hole had a nominal diameter of 0.250 in.

5. THEORETICAL AND EXPERIMENTAL RESULTS

Residual strains were obtained with 7075-T6 aluminum. The computed and experimental values are shown in Figs. 4, 5, and 6, for radial expansions of 0.0095, 0.004, and 0.002 in., respectively. The plots show excellent agreement between theoretical and experimental values of hoop strain. The corresponding hoop and radial stresses from the theory are shown in Figs. 7 and 8. Both the hoop and radial residual stresses are compressive near the hole for the three cases of radial displacement.

An important characteristic of these results is that the peak positive (tension) hoop stress remains almost constant at $\frac{\sigma_\theta}{\sigma_y} = 0.4$. An excessive level of σ_θ would lead to accelerated failure when tension loads are applied. The position of the peak, however, increases radially, away from the hole, as the same specimens with the rivet removed are shown in Figs. 9, 10, and 11. Comparison of experimental and theoretical results for one case of an open hole (i.e., $\Delta R = 0.0045$ in.) shows good agreement (see Fig. 12).

In another set of calculations and experimental measurements, 2024-T3 material was used with A-286 rivets. The results are shown in Figs. 13, 14, and 15, (i.e., $\Delta R = 0.011$ in.). The case of 2024-T3 specimens with the rivet removed is shown in Figs. 16, 17, and 18.

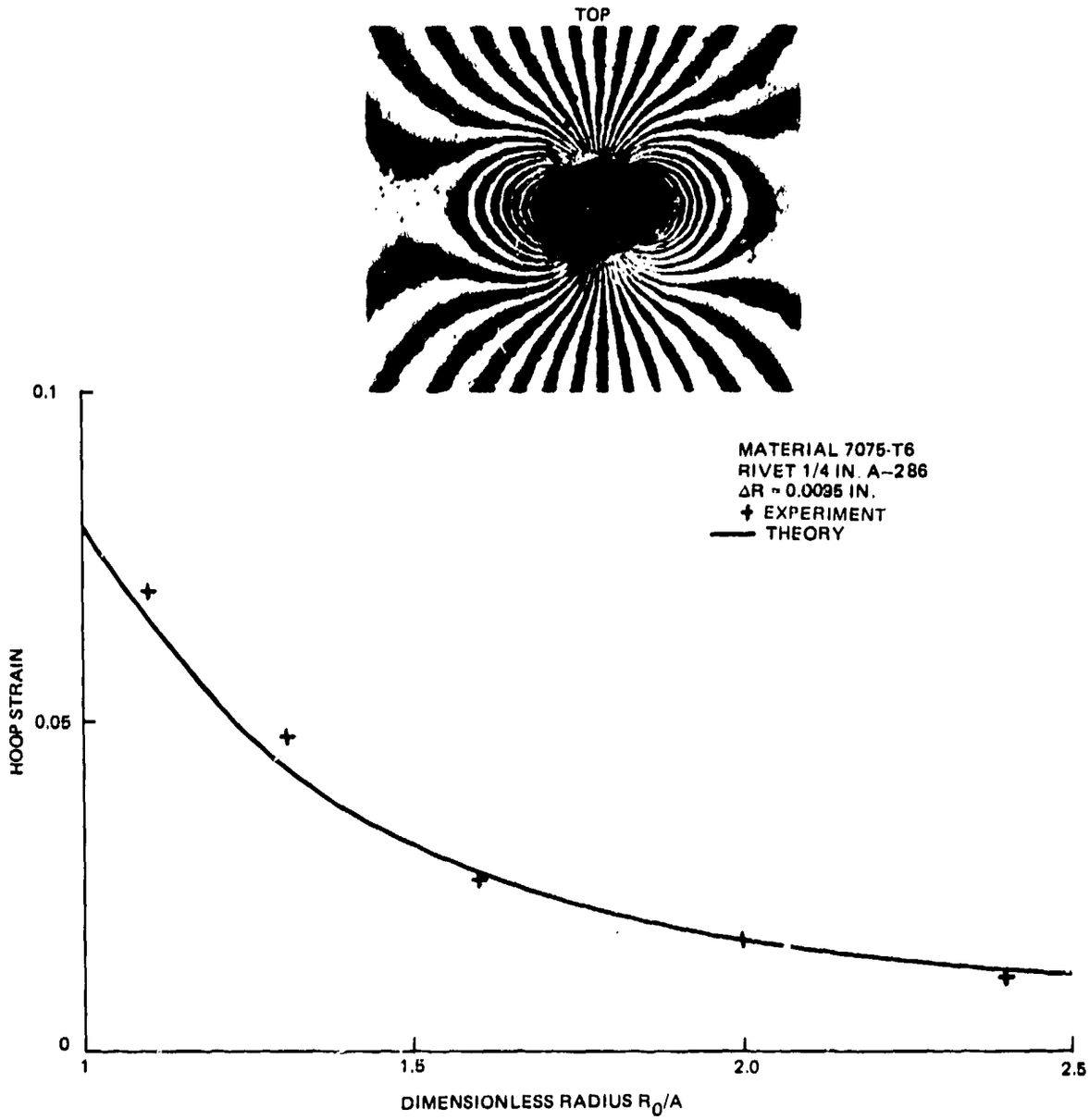

Fig. 4 Residual Hoop Strain vs Radial Distance, ΔR=0.0095 In Radial Expansion

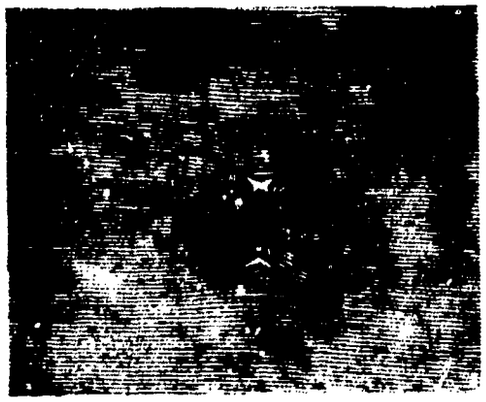

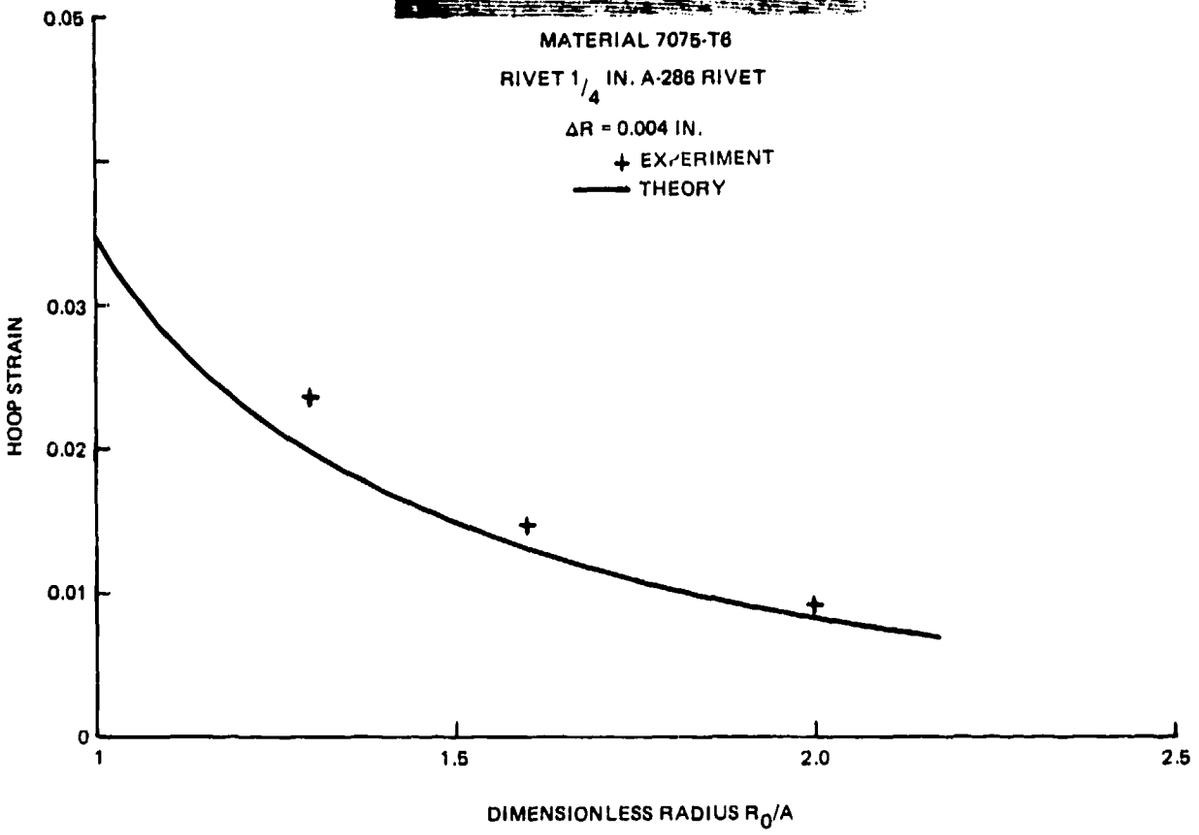

Fig 5 Residual Hoop Strain vs Radial Distance, ΔR = 0.004 In. Radial Expansion

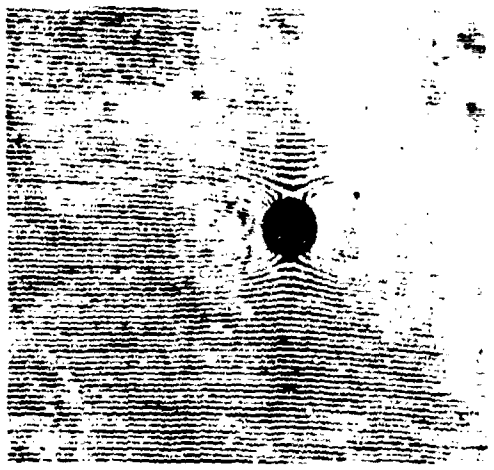

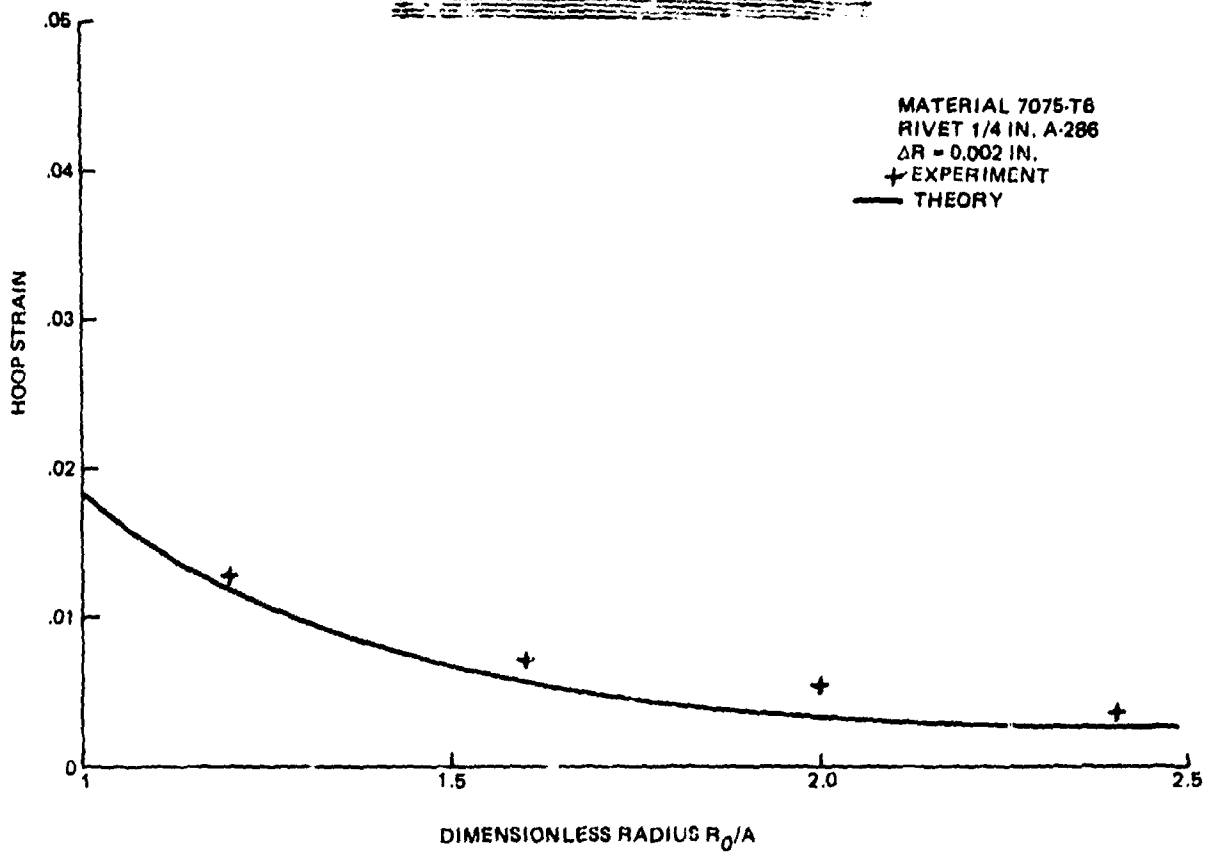

Fig. 6 Residual Hoop Strain vs Radial Distance, ΔR = 0.002 In. Radial Expansion

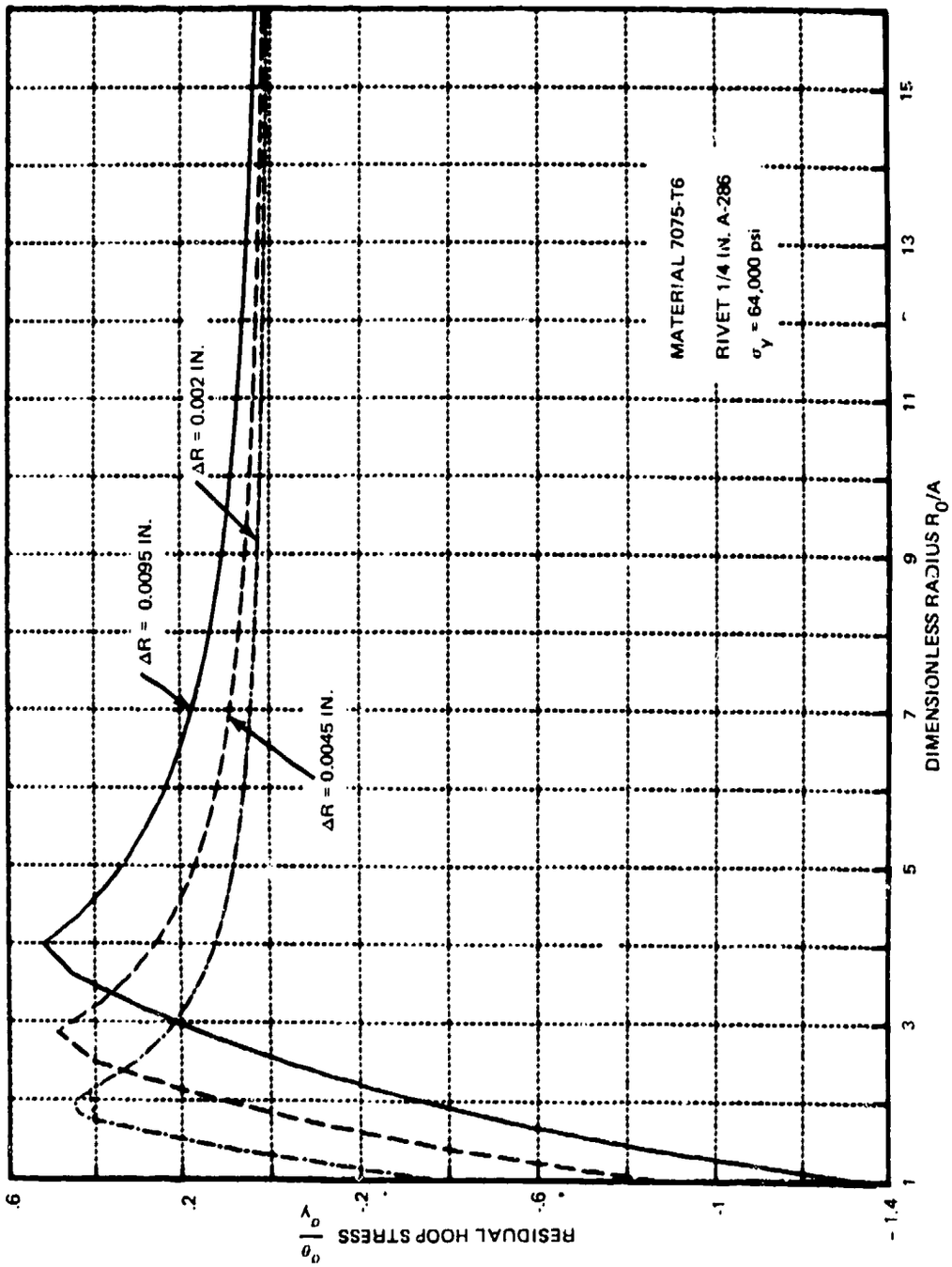

Fig. 7 Residual Hoop Stress vs Radial Distance

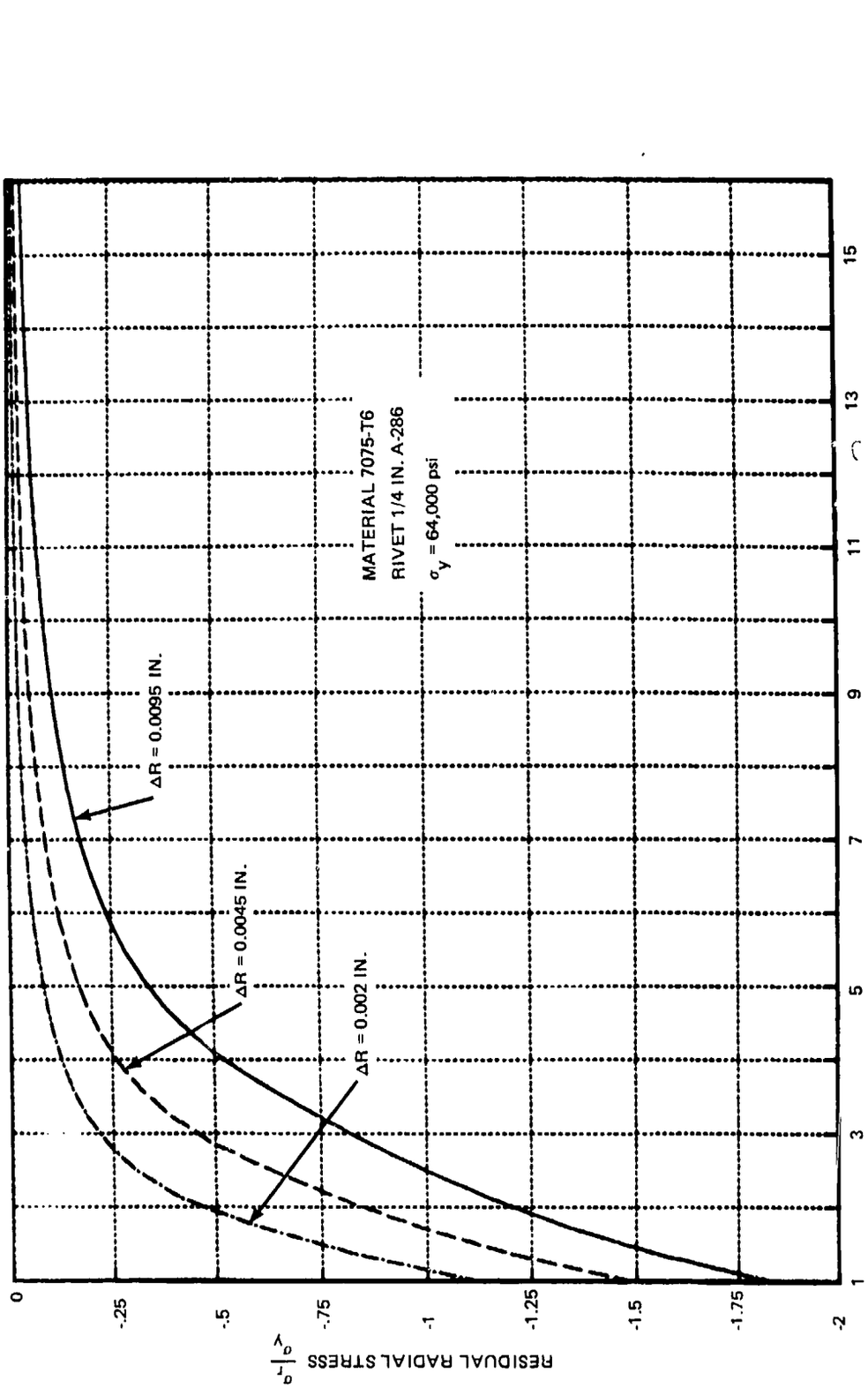

Fig. 8 Residual Radial Stress vs Radial Distance

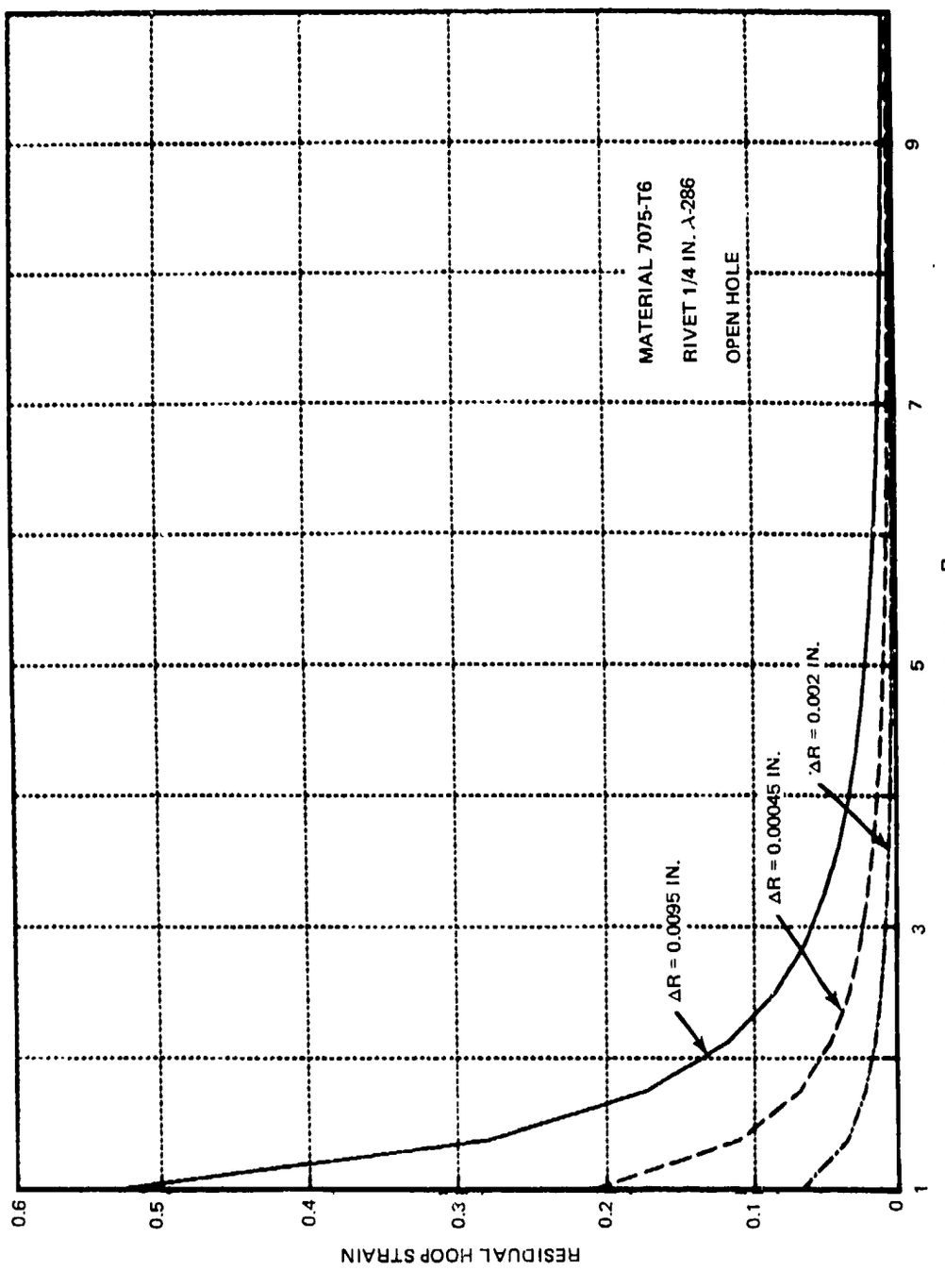

Fig. 9 Residual Hoop Strain vs Radial Distance

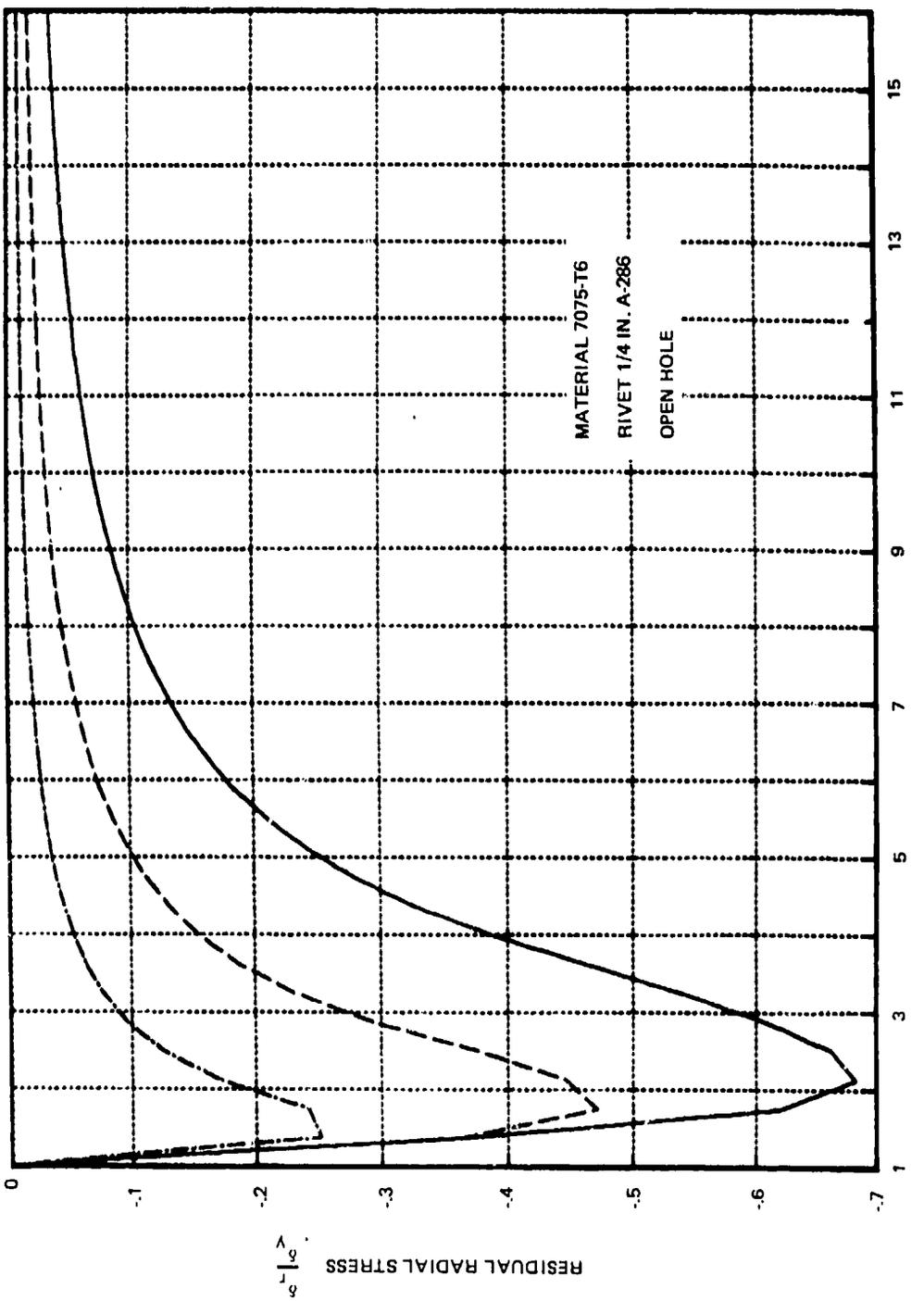

Fig. 10 Residual Radial Stress vs Radial Distance

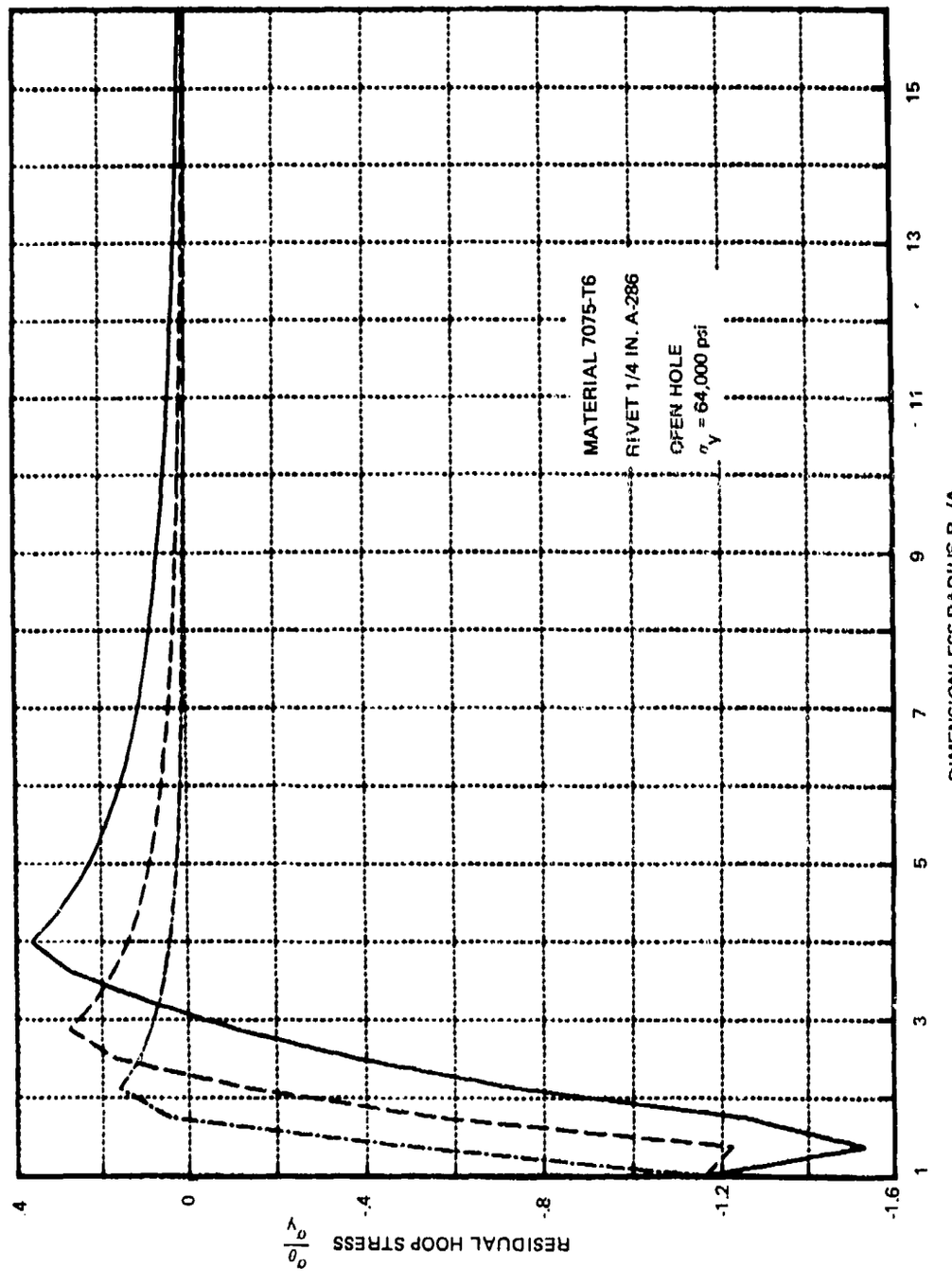

Fig. 11 Residual Hoop Stress vs Radial Distance

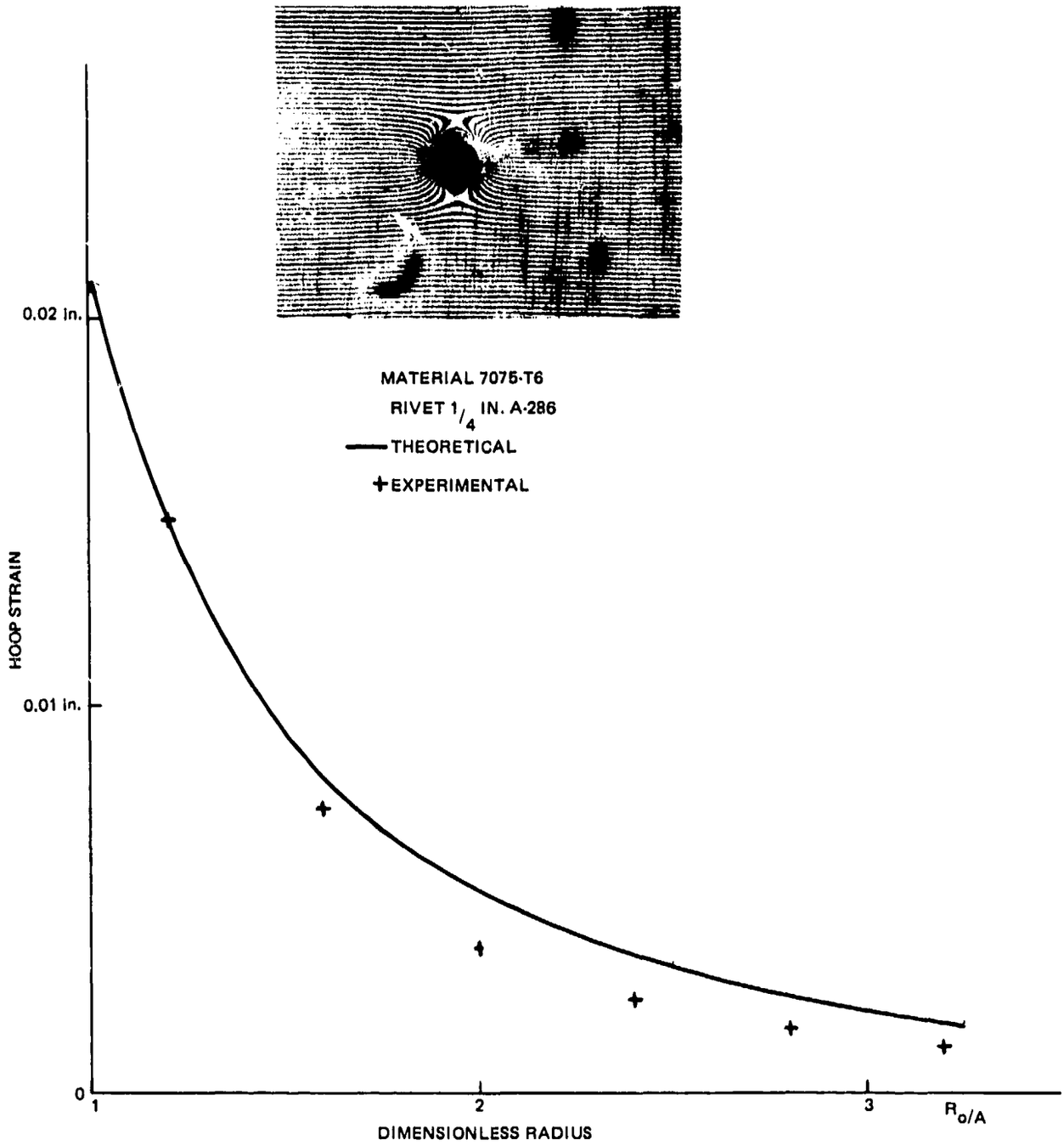

Fig. 12 Residual Hoop Strain vs Radial Distance, Open Hole (Rivet Removed After Expansion)

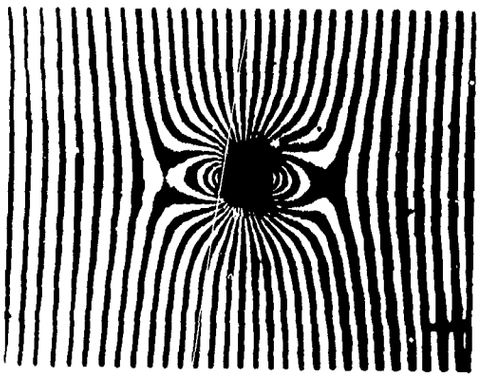

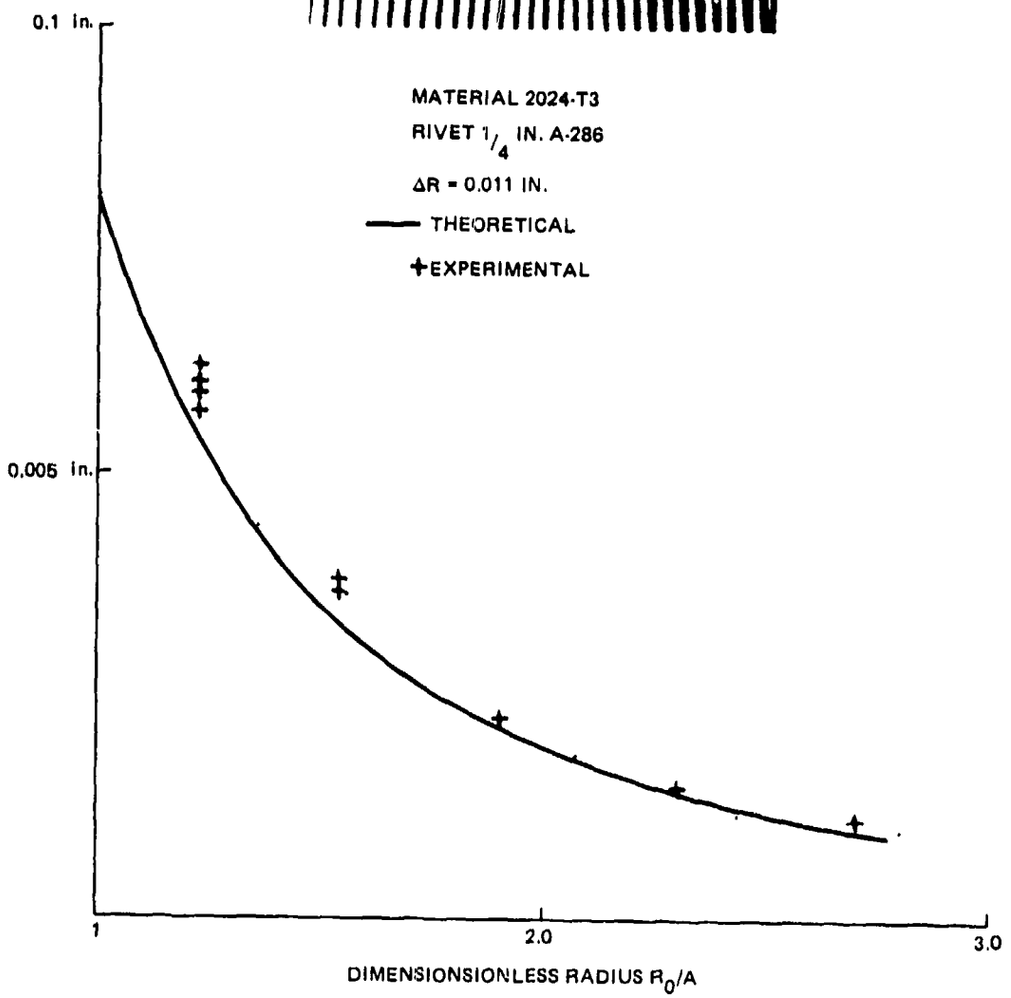

Fig. 13 Residual Hoop Strain vs Radial Distance, ΔR = 0.011 Radial Expansion

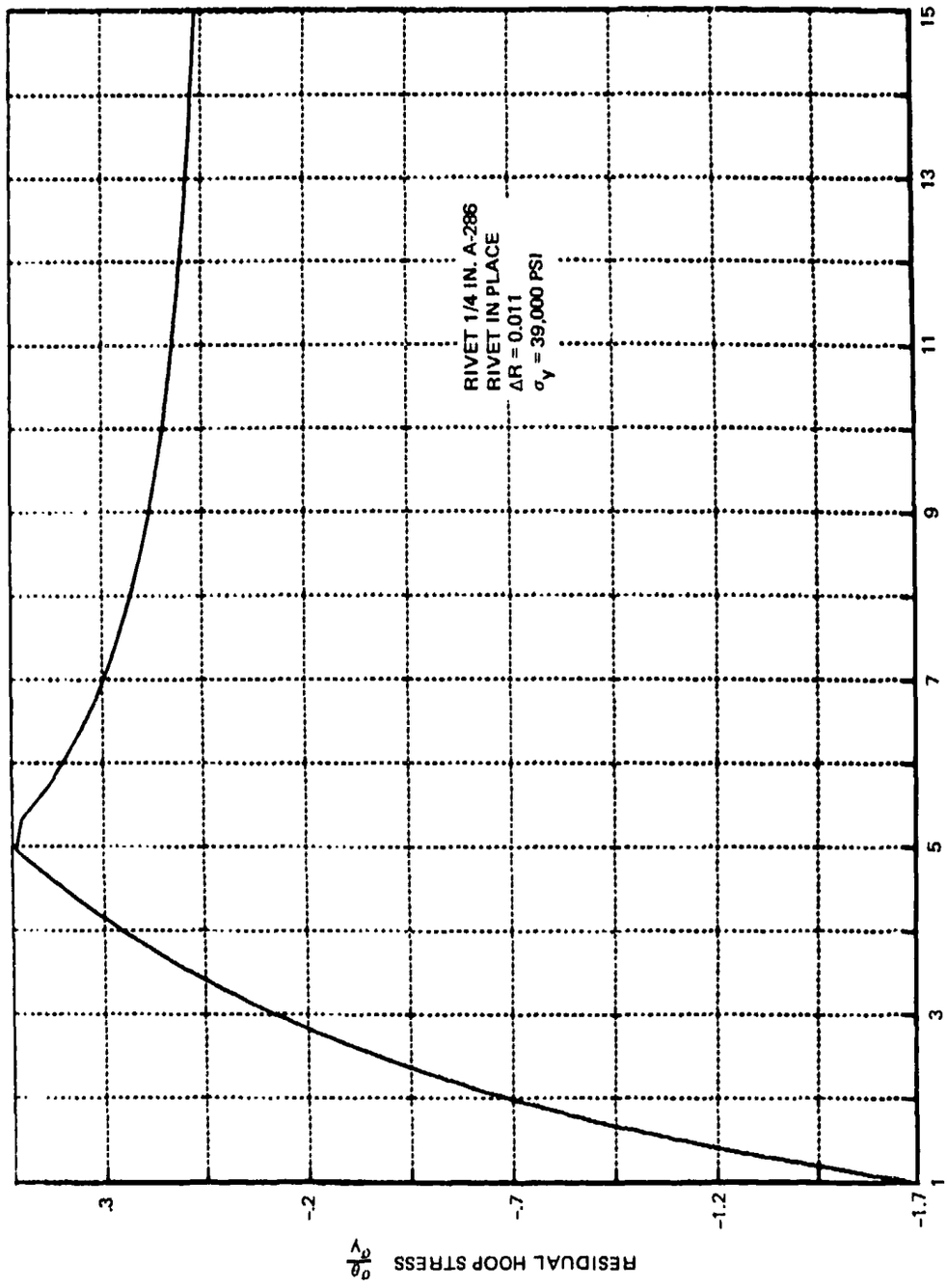

Fig. 14 Residual Hoop Stress vs Radial Distance, AL 2024-T3

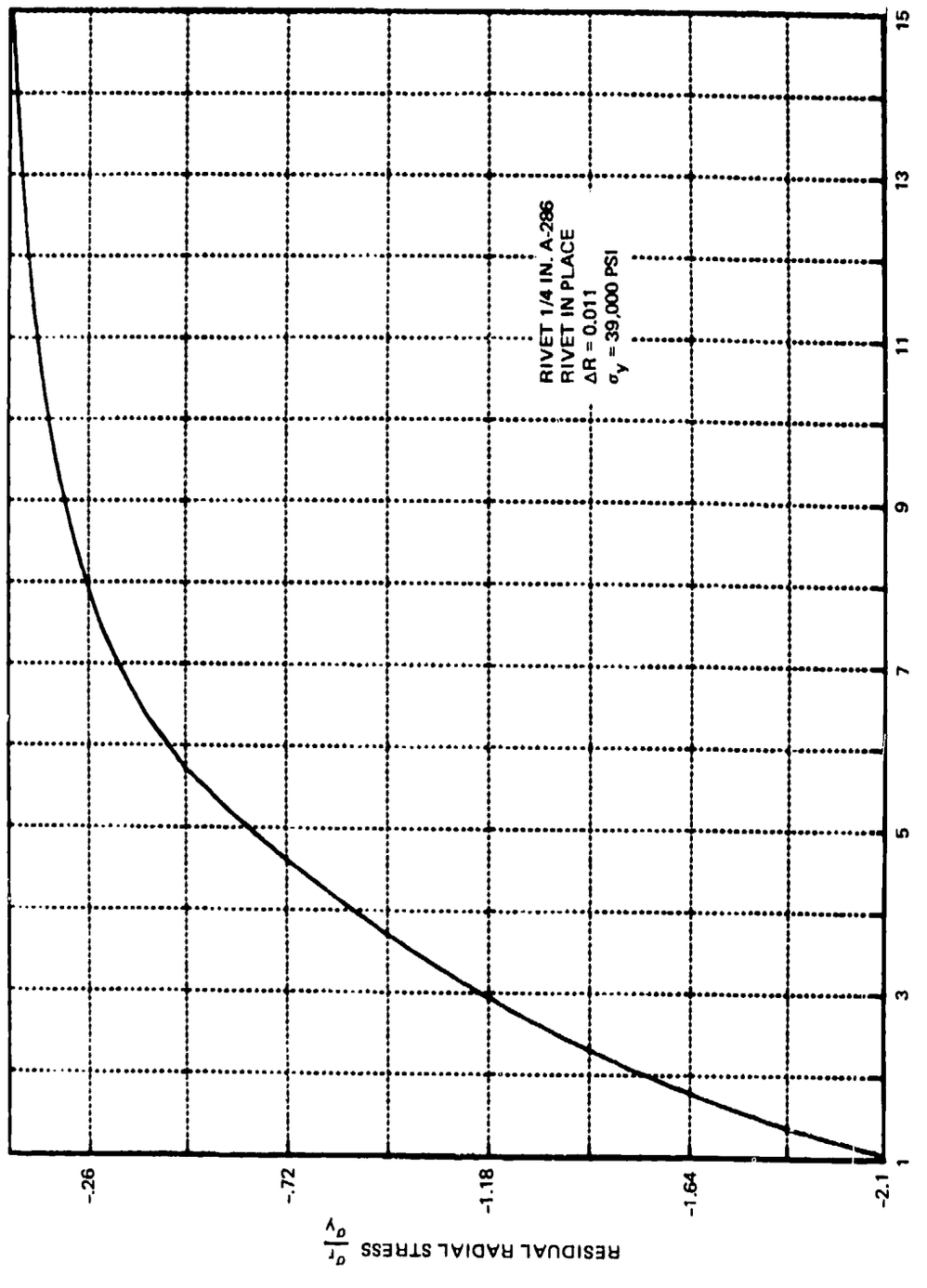

Fig. 15 Residual Radial Stress vs Radial Distance, AL 2024-T3

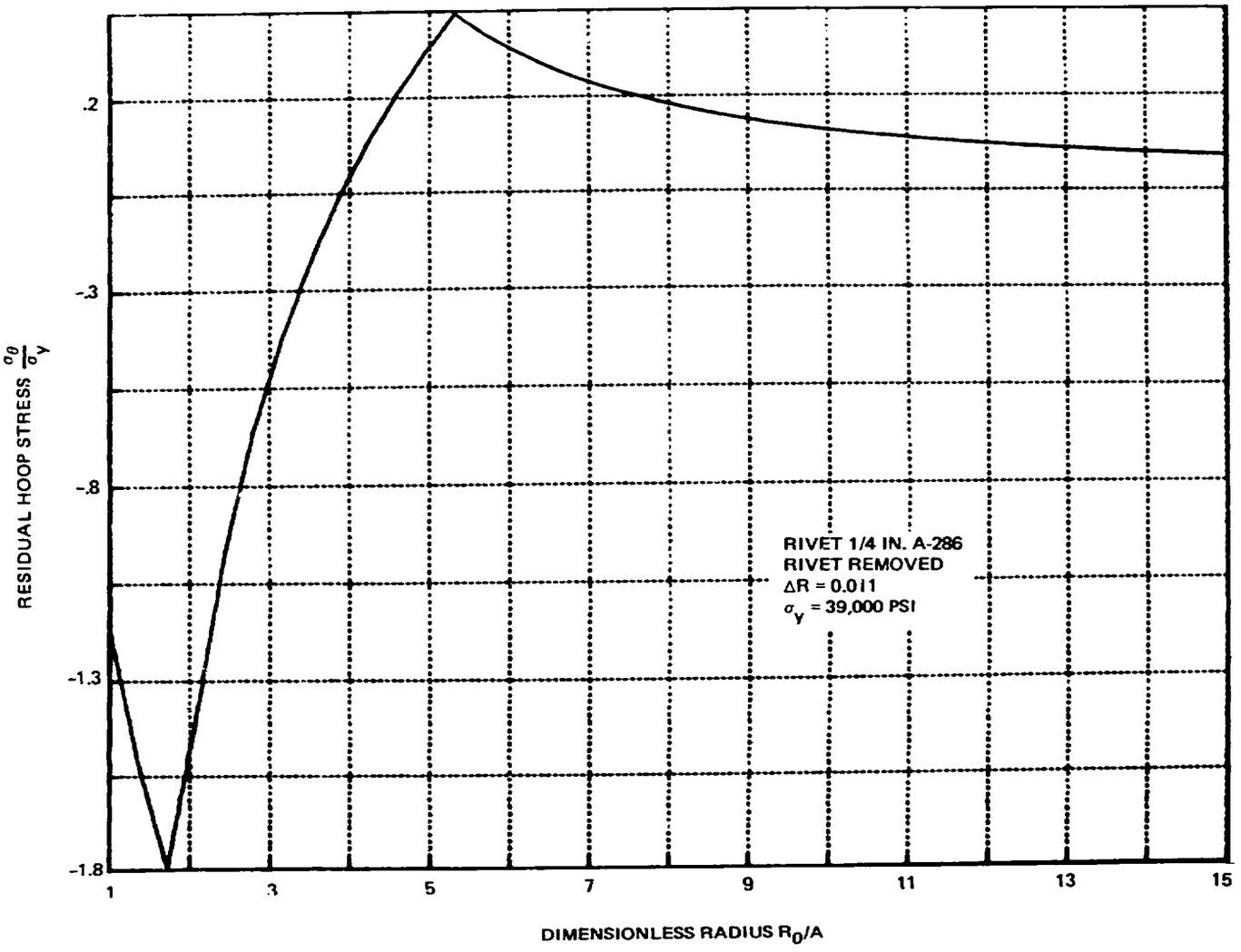

Fig. 16 Residual Hoop Stress vs Radial Distance, AL 2024-T 3

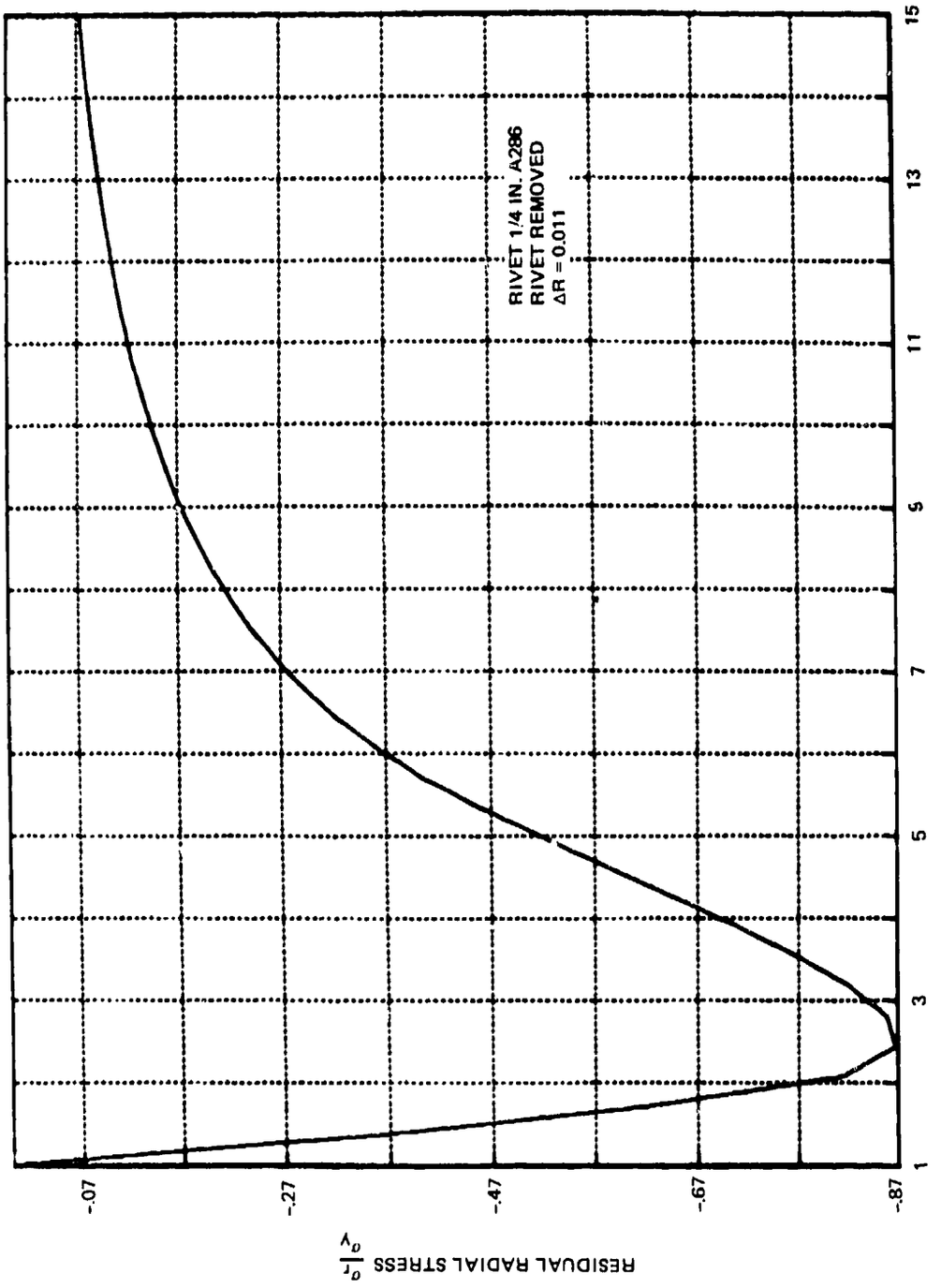

Fig. 17 Residual Radial Stress vs Radial Distance, AL 2024-T3

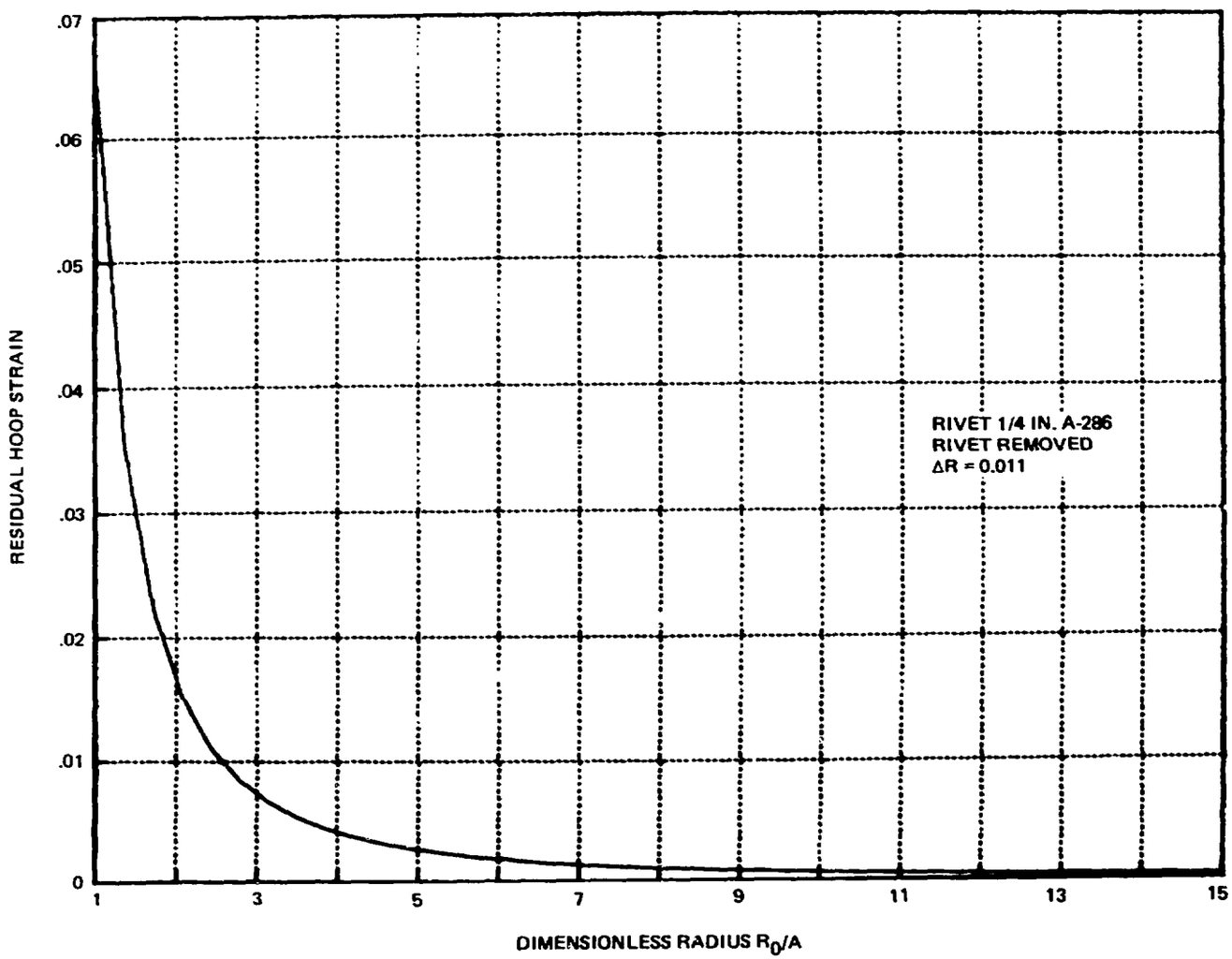

Fig. 18 Residual Hoop Strain vs Radial Distance, AL 2024-T3

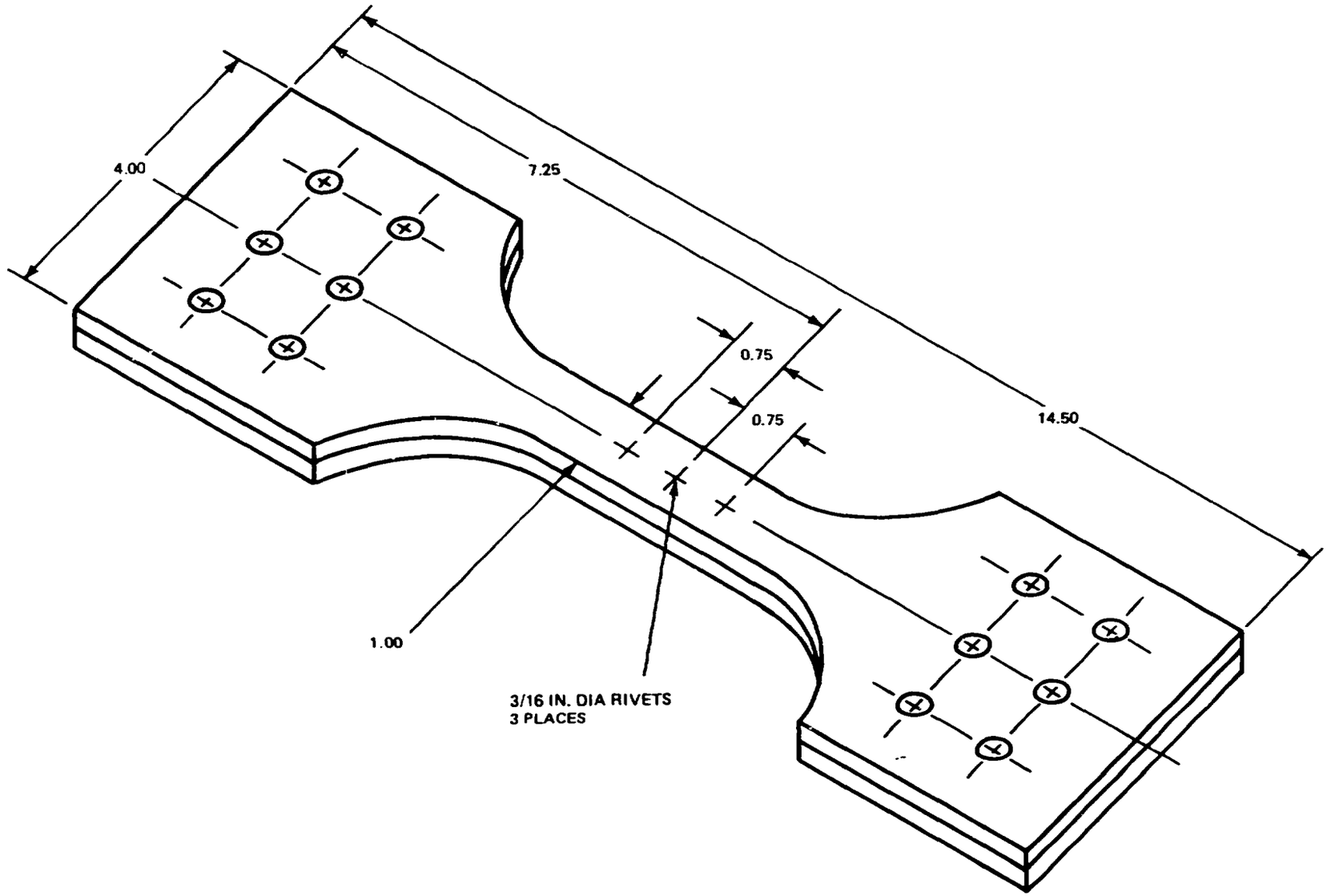

Fig. 19 Two-Piece Laminated Fatigue Specimen Configuration With Unloaded Fasteners

6. CONSTANT AMPLITUDE FATIGUE TESTS OF SPECIMENS WITH RESIDUAL STRESSES

When residual stresses are combined with applied stresses due to a uniaxially applied load in a specimen, they directly affect the fatigue life of the specimen. To illustrate this effect specimens made of 2024-T87 material were used. In the first series of tests specimens whose geometry is shown in Fig. 19 were made each with three open holes of 0.188 in. diameter. They were tested at constant amplitude and the results, along with previous results, are shown in Fig. 20.*

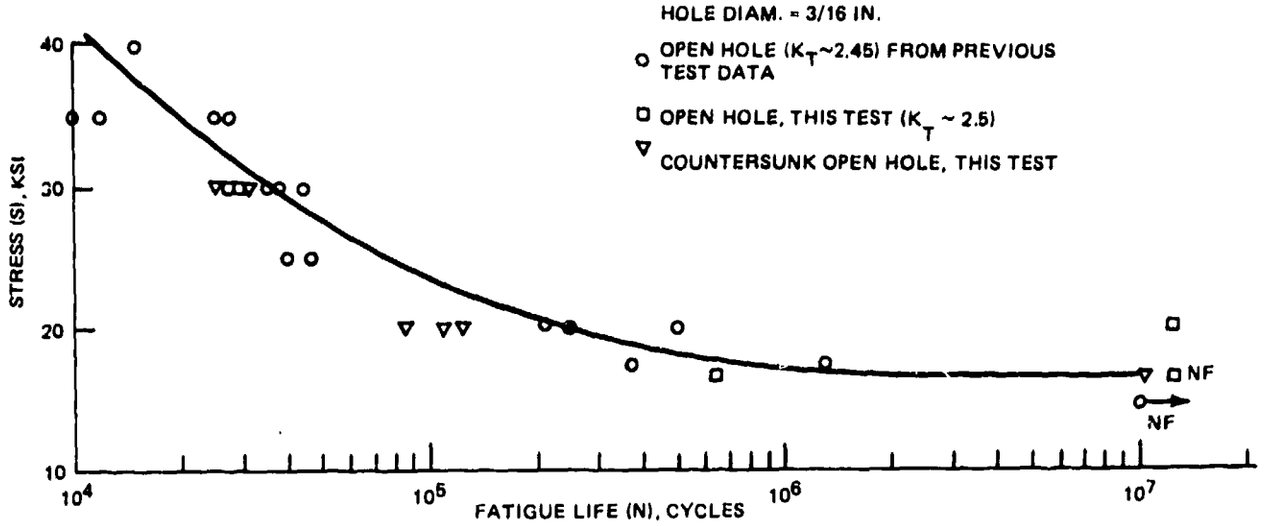

Fig. 20 Fatigue Life of 2024-T81 Aluminum Alloy Open Hole and Countersunk Open Hole Control Specimens

---

* Note: Grumman Report MPLR 45-76-23, "Constant Amplitude Fatigue Test Results of Cracked and Uncracked 2024-T81 Aluminum Alloy Containing "Unloaded" Stress Wave Driven Rivets," Materials and Process Department, 19 May 1977.

In the second series of tests the specimens were drilled with the same holes and riveted with the Stress Wave Riveter using three different types of rivets; 2117-T4, A-286 (GR-501W-6), and Beta C titanium. The specimens were again tested at constant amplitude at two stress levels, 30 ksi and 20 ksi. The results are shown in Figs. 21, 22, and 23. The radial displacement was 0.005 and 0.006 in. in each case.

The important conclusion from this limited number of specimens is that regardless of rivet material, the improvement in fatigue life, when compared to open hole results, is about ten times that of the open hole specimens. More extensive testing is required to arrive at more definitive conclusions. It is also important to find some theoretical mechanism to predict life once the initial residual stresses and the load are known. A modified Goodman's diagram may be suitable.

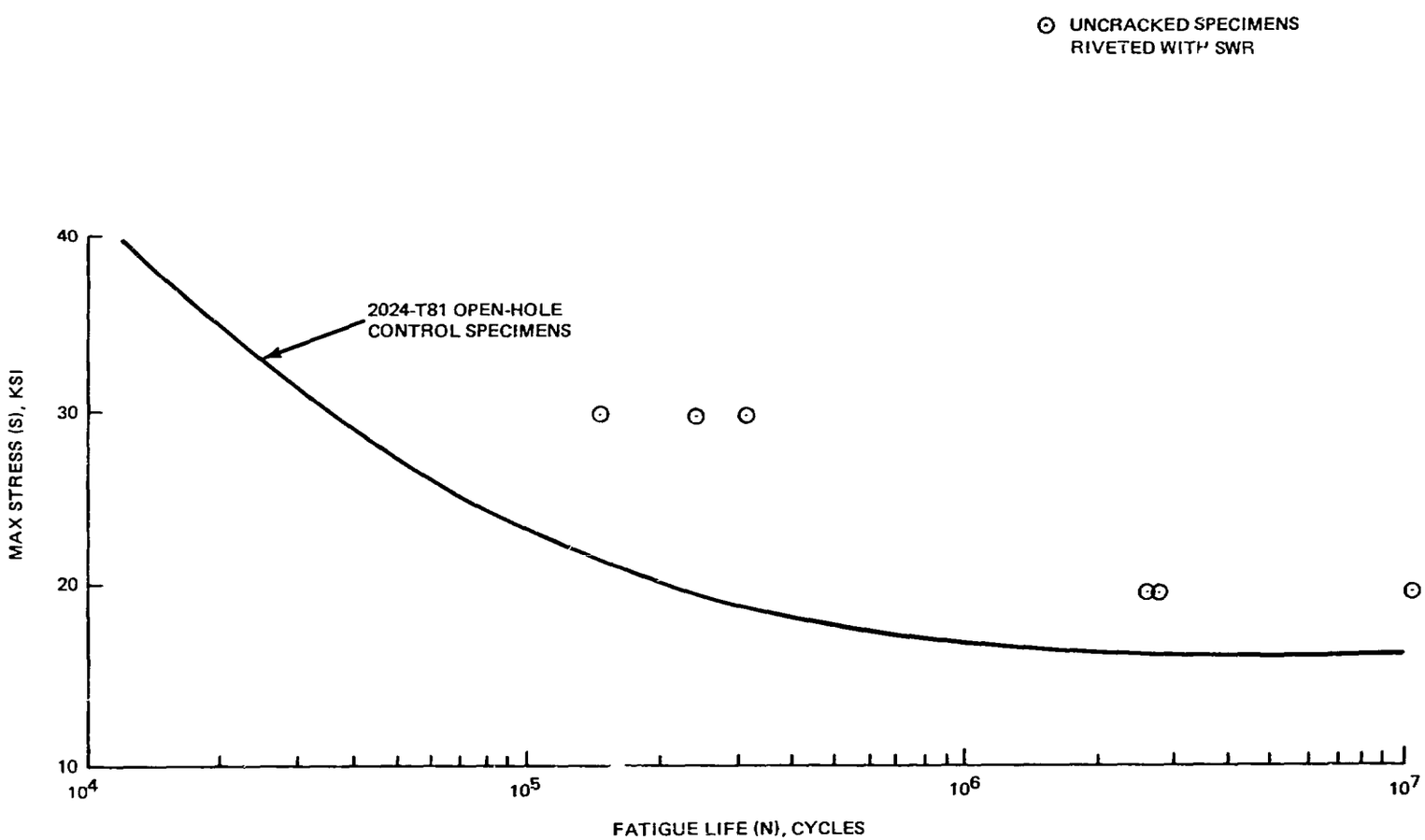

Fig. 21 Fatigue Life of 2024-T81 Aluminum Alloy Specimens Containing Unloaded 3/16 In. Dia 2117-T4 Aluminum Rivets Installed with Stress Wave Riveter

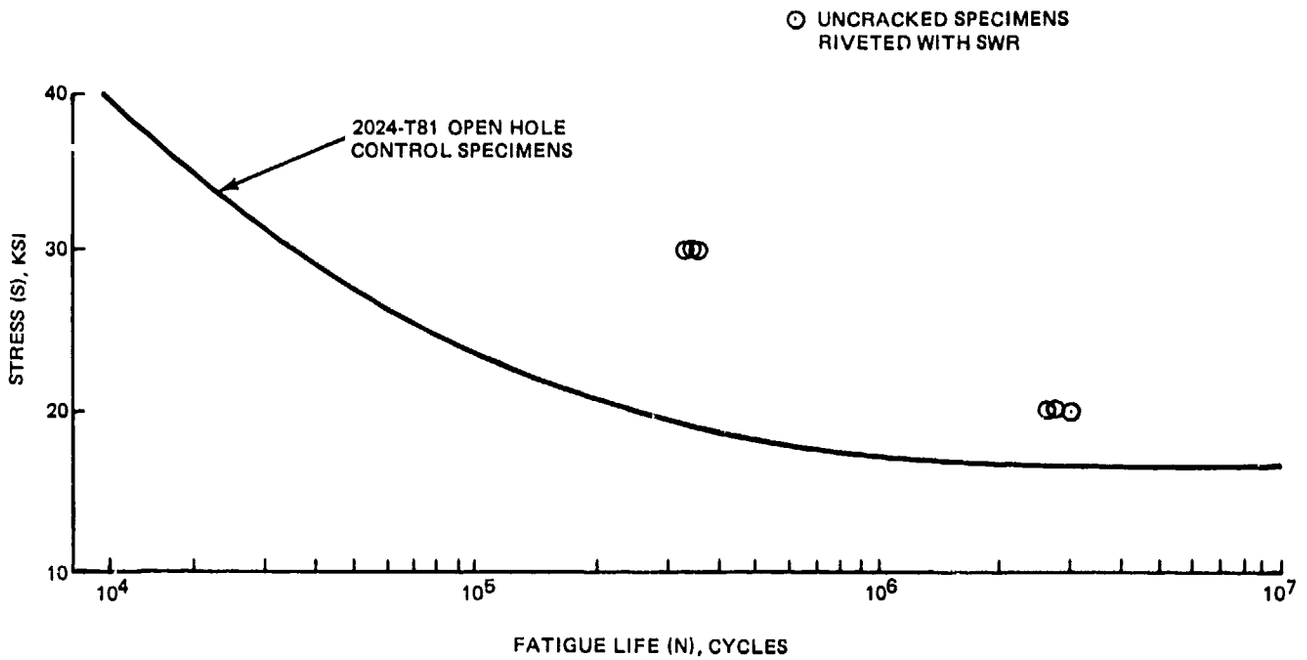

Fig. 22 Fatigue Life of 2024-T81 Aluminum Alloy Specimens Containing Unloaded 3/16 In. Dia A-286 Steel Rivets Installed with Stress Wave Riveter.

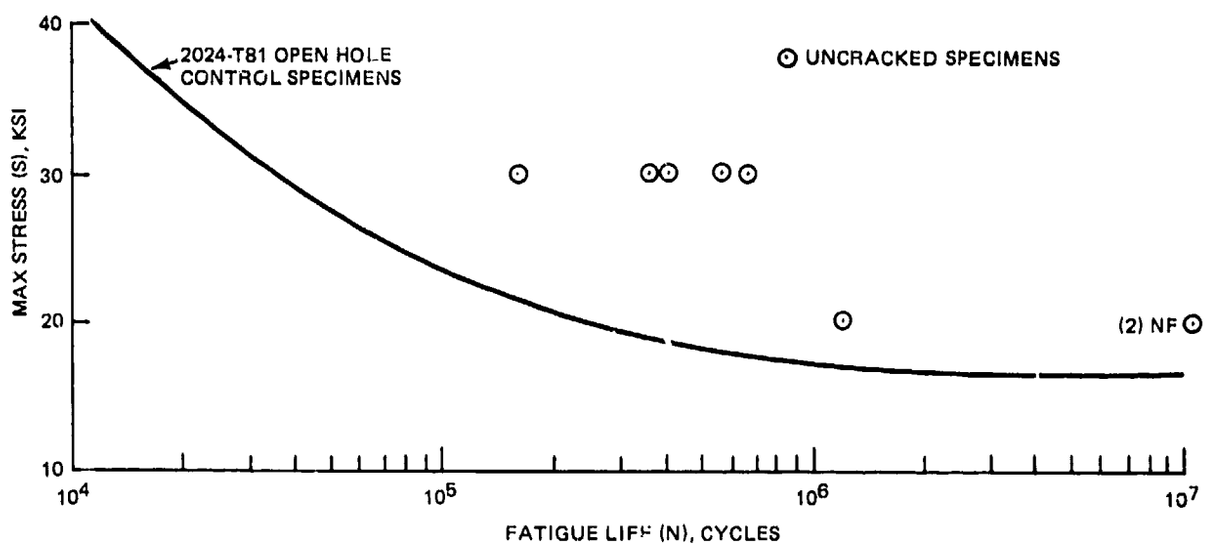

Fig. 23 Fatigue Life of 2024-T81 Aluminum Alloy Specimens Containing Unloaded 3/16 In. Dia Beta C Titanium Rivets Installed with Stress Wave Riveter

7. EFFECT OF PRECRACKED HOLES ON FATIGUE LIFE OF DYNAMICALLY RIVETED SPECIMENS

A radial crack in a hole surface, where stress concentration is high, provides the most favorable conditions for failure. To show the beneficial effect of dynamic riveting using the Stress Wave Riveter, we tested specimens with precracked holes.

The specimens were of the same design as described in Section 6. Pilot holes of $\frac{1}{8}$ in. were first drilled and the specimens were subjected to constant amplitude fatigue until a radial crack was developed in a preassigned notched area. The holes were then drilled and countersunk to $\frac{3}{16}$ in. diameter, with the crack in each hole of 0.05 in. measured to within 0.005 in. and extended through the thickness of the countersunk part. (Each specimen consisted of two parts, $\frac{1}{8}$ in. thick each made of 2024-T81 material.)

The Stress Wave Riveter was used to install rivets made of (a) modified Beta C Titanium rivets (b) 2117-T4 aluminum rivets, and (c) A-286 rivets. The nominal radial expansion was 0.006 in. in each case.

The specimens were tested at constant amplitude load cycling.* The results are shown in Fig. 24. The specimens riveted with A-286 show the best improvement when compared to the fatigue life of open hole precracked specimens. It is apparent, however, that all the riveted specimens, with compressive residual

---

* Note: Grumman Report MPLR-45-77-135, "Open Hole Precracked Specimens Tested at Constant Amplitude Load Cycling," Materials and Process Department, October 1977.

stresses, improved fatigue life and otherwise slowed the crack growth. The fatigue life of each riveted specimen was approximately ten times greater than the open hole precracked specimens.

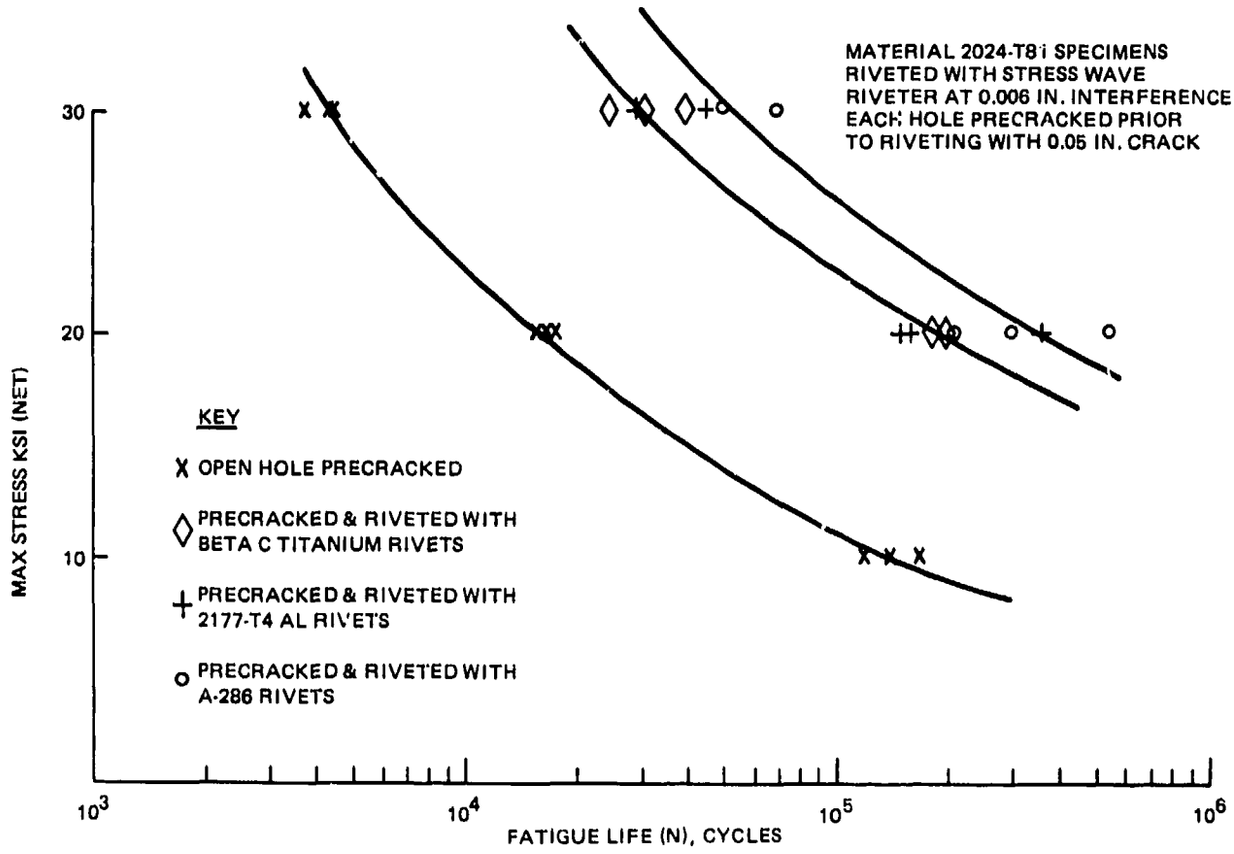

Fig. 24 Constant Amplitude Load Cycling Fatigue Tests of Specimens Riveted with Stress Wave Riveter

8. DISCUSSION OF RESULTS

The plane strain assumption made in the analysis has given results that agree well with tests. It must be remembered, however, that the specimens used with the Moiré technique were $\frac{1}{4}$ in. thick and were protected during riveting on either side by $\frac{1}{8}$ in. plates. Metallographic analysis shows that near the surface plane stress conditions prevail. These conditions were removed with the protective plates. The plane strain conditions therefore are not valid in thin sheets, less than 0.06 in. thickness, where the present analysis may not be applicable.

The plane strain condition, of course, is accompanied by axial stresses as shown in Appendix E. With the rivet in place, triaxial stresses exist near the hole surface. When the rivet is removed, however, we have only hoop and axial residual stresses. These conditions can be used with a modified Goodman's diagram to predict fatigue life.

The incompressibility assumption was essential in the development of the theoretical analysis. Prager and Hodge (Ref. 8) argue that, "the assumption, which greatly facilitiates the mathematical work, furnishes good results if the corrections 2μ and $2(1-\mu)$ are applied to the axial stress and the radial displacement, respectively". They arrived at these factors by comparing theoretical solutions of compressible and incompressible materials in static loading. Since we are comparing the incompressible solution with experimental results in dynamic loading we believe that any discrepancies are within the errors of computation and therefore no correction factors are needed.

The radial and hoop stress solutions between compressible and incompressible materials should agree well according to Prager and Hodge.

The Moiré technique used to measure residual strains proved successful enough to recommend it for practical applications. Despite early difficulties with fringes disappearing near the hole, the final quality of the fringe reproduction is excellent. Our innovative technique of protective plates during riveting was imperative for the protection of thin film near the hole.

In conclusion, the results of this work show that there is a triaxial residual stress field around the hole that is induced by dynamically expanding the rivet in the hole. Furthermore, the radial extent of cold-work is at least as much as that provided by other cold-work methods such as the sleeve and the split sleeve techniques. In addition, it is shown that the residual stresses do improve fatigue life. Comparison of fatigue data shows that for constant amplitude cyclic loading and 0.006 in. radial expansion of cold-work we obtain an increase of 10 times the fatigue life of specimens without the cold-work. What is more important, however, is that residual stresses induced around a precracked hole by the dynamically expanding rivet slow down the crack propagation and improve fatigue life.

9. REFERENCES

1. Dietrich, G. and Potter, J. M., "Stress Measurements in Cold-Worked Fastener Holes: Advances in X-Ray Analysis," Vol. 20, 1977.

2. Chang, J. B., "Prediction of Fatigue Crack Growth Cold-Worked Fastener Holes," AIAA, Vol. 14, no. 9, Sept. 1977.

3. Seely, M. S. and Smith, A. M., Advanced Mechanics of Materials, John Wiley & Sons, Publishers, 1952.

4. Leftheris, B. P., "Stress Wave Analysis," Grumman Research Department Report, RE-503, 1975.

5. Adler, W. F., Dupree, D. M., "Stress Analysis of Cold-Worked Fastener Holes," AFML-TR-74-44, July 1974.

6. Armen, H., Pifko, A. and Levine, H. S., Finite Element Analysis of Structures in the Plastic Range, NASA CR-1649, February 1971.

   as used in

   Crews, J. H., Jr., "Analytical and Experimental Investigation of Fatigue in a Sheet Specimen with an Interference-Fit Bolt," NASA TN-D-7926, July 1975.

7. Mendelson, A., Plasticity: Theory and Application, McMillan, 1968.

8. Prager, W. and Hodge, P. G., Jr., Theory of Perfectly Plastic Solids, Dover Publications, 1950.

9. Davies, R. M., "A Critical Study of the Hopkinson Pressure Bar," Philosophical Transactions Series A-240, p. 375, Royal Scoiety of London, 1948.

APPENDIX A

DERIVATION OF STRAIN RELATIONS

DEFINITION OF STRAINS

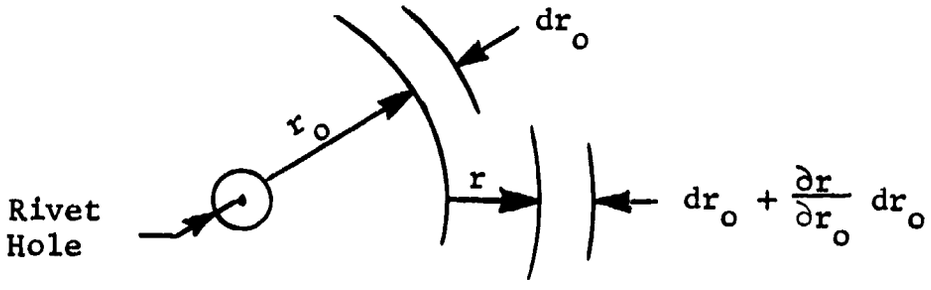

Radial Strain:
$$\epsilon_r = \frac{(dr_o + \frac{\partial r}{\partial r_o} dr_o) - dr_o}{dr_o} = \frac{\partial r}{\partial r_o} \qquad \text{(A-1)}$$

Hoop Strain:
$$\epsilon_\theta = \frac{(r + r_o) - r_o}{r_o} = \frac{r}{r_o} \qquad \text{(A-2)}$$

Volumetric change:
$$e = \epsilon_r + \epsilon_z + \epsilon_\theta \qquad \text{(A-3)}$$

RELATIONS WITH MEAN NORMAL STRESS

From Hook's law we have:

$$\sigma_r = \frac{3\mu E}{(1+\mu)(1-2\mu)} e + \frac{E}{1+\mu} \epsilon_r$$

$$\sigma_\theta = \frac{3\mu E}{(1+\mu)(1-2\mu)} e + \frac{E}{1+\mu} \epsilon_\theta$$

$$\sigma_z = \frac{3\mu E}{(1+\mu)(1-2\mu)} e + \frac{E}{(1+\mu)} \epsilon_z$$

where

$$e = \frac{\epsilon_r + \epsilon_\theta + \epsilon_z}{3}$$

Adding the three stress equations we obtain

$$(\sigma_r+\sigma_z+\sigma_\theta) = 3 \frac{3\mu E}{(1+\mu)(1-2\mu)} e + \frac{E}{(1+\mu)} (\epsilon_r+\epsilon_z+\epsilon_\theta) .$$

Since

$$k = \frac{E}{3(1-2\mu)}$$

and

$$\epsilon_r + \epsilon_z + \epsilon_\theta = 3e$$

we have

$$\frac{(\sigma_r+\sigma_z+\sigma_\theta)}{3} = \frac{9\mu\ ke}{(1+\mu)} + \frac{3(1-2\mu)\ ke}{(1+\mu)} .$$

From the definition of the stress deviator we have

$$S = \frac{\sigma_r+\sigma_z+\sigma_\theta}{3} = 3ke \qquad \text{(A-4)}$$

From the definition of the principal stresses, we have

$$\sigma_r = S + S_r , \quad \sigma_\theta = S + S_\theta \quad \text{and} \quad \sigma_z = S + S_z$$

Adding the three equations we obtain

$$(\sigma_r + \sigma_\theta + \sigma_z) = 3S + (S_r + S_\theta + S_z).$$

From Eq. (A-3), however, we have $\sigma_r + \sigma_\theta + \sigma_z = 3S$.

Thus, we conclude with

$$S_r + S_\theta + S_z = 0 \qquad \text{(A-5)}$$

RELATIONS BETWEEN STRESS AND STRAIN DEVIATORS

From Hook's law we have

$$\sigma_r = \frac{9\mu}{(1+\mu)} K \cdot e + \frac{E}{(1+\mu)} \epsilon_r$$

or

$$\sigma_r - S = \frac{3\mu}{(1+\mu)} (3Ke) - S + \frac{E}{(1+\mu)} \epsilon_r .$$

Substituting for S from Eq. (A-4) in the right hand side and $k = \frac{E}{3(1-2\mu)}$, we obtain

$$\sigma_r - S = \frac{E}{(1+\mu)} (\epsilon_r - e)$$

Introducing incompressibility, where $e = 0$, we obtain

$$S_r = \sigma_r - S = \frac{E}{1+\mu} \epsilon_r = E' \epsilon_r$$

Similarly,

$$S_\theta = \sigma_r - S = \frac{E}{1+\mu} \epsilon_\theta = E' \epsilon_\theta \qquad \text{(A-6)}$$

and

$$S_z = \sigma_z - S = \frac{E}{1+\mu} \epsilon_z = E' \epsilon_z$$

APPENDIX B

DERIVATION OF EQUATIONS OF STRESS AND STRAIN DISTRIBUTION DURING ELASTIC LOADING

It is possible to integrate each of Eqs. (13) separately and evaluate the constants from the boundary conditions. Integrating the second equation in (13) we obtain $u = \frac{C_1(t)}{r_o}$, and from the boundary conditions of the hole surface $u = u_o = mt$ at $r_o = a$, we obtain a general solution for the velocity

$$u = \frac{mt \cdot a}{r_o} \tag{B-1}$$

Integrating the compatibility equation (Eq. (2)) with respect to r_o using Eq. (3) with $\epsilon_z = 0$, we also obtain

$$\epsilon_\theta = \frac{C_2(t)}{r_o^2}$$

Since at $r_o = a$, $u = mt$ we obtain $\dot{\epsilon}_\theta(a) = \frac{mt}{a}$ from Eq. (4).

Hence $C_2(t) = \dot{\epsilon}_\theta(a)\, a^2 = mta$, and $C_2(t) = \frac{mt^2 a}{2}$, since at $t = 0$, $\epsilon_\theta = 0$ and $C_2(o) = 0$.

The equation for ϵ_θ is, therefore, given by

$$\epsilon_\theta = \frac{mt^2 a}{2r_o^2}$$

and employing the plane strain condition where $\epsilon_r = -\epsilon_\theta$, we obtain

$$\epsilon_r = \frac{mt^2 a}{2r_o^2} \tag{B-2}$$

The first equation of (13) can now be reduced to a simpler form. Using Eq. (10a), we can write

$$\frac{\rho ma}{r_o} + \frac{\partial S}{\partial r_o} = - \frac{1}{r_o^2} \frac{\partial (S_r r_o^2)}{\partial r_o}$$

Substituting in Eq. (10) for ϵ_r and ϵ_θ we obtain

$$S_r = - \frac{E^1 m t^2 a}{2 r_o^2}$$

Multiplying by r_o^2 and differentiating we obtain

$$\frac{\partial}{\partial r_o} (S_r r_o^2) = 0$$

Thus,

$$\frac{\partial S}{\partial r_o} + \frac{\rho ma}{r_o} = 0$$

or

$$\frac{\partial S}{\partial r_o} = - \frac{\rho ma}{r_o} \qquad \text{(B-3)}$$

Integrating Eq. (B-3) we have

$$S = - \rho ma \, \ell n \, r_o + C_3(t)$$

Where $C_3(t)$ is the constant of integration.

We finally find an expression for S, using the boundary condition of $S = 0$ at all times when $r_o = b$ where $b \gg a$.

$$S = \rho ma \, \ell n \frac{b}{r_o} \qquad \text{(B-4)}$$

Substituting Eqs. (10) and (B-4) in Eq. (7), we obtain the final equation of stress and strain for the elastic case.

$$\left.\begin{aligned} \sigma_r &= \rho ma \, \ell n \frac{b}{r_o} - \frac{E' mt^2 a}{2r_o^2} \\ \sigma_\theta &= \rho ma \, \ell n \frac{b}{r_o} + \frac{E' mt^2 a}{2r_o^2} \\ \epsilon_r &= -\frac{mt^2 a}{2r_o^2} \end{aligned}\right\} \qquad \text{(B-5)}$$

and

$$\epsilon_\theta = \frac{mt^2 a}{2r_o^2}$$

APPENDIX C

SOLUTION OF CONSTANT VELOCITY REGION

Tests show (see Fig. 2) that when the rivet impacts the hole surface, there is a momentary reversal in velocity change, from acceleration to deceleration. When acceleration begins again, it takes time t_o reach a constant velocity. Then the velocity remains constant for the time interval $(t_2 - t_o)$. During this interval the acceleration is zero and the velocity at $r_o = a$ is $u = u_o$.

$$\epsilon_r + \epsilon_\theta = \frac{\partial r}{\partial r_o} + \frac{r}{r_o} = 0 \text{ (incompressibility)}$$

differentiating w.r.t. time we obtain

$$\dot{\epsilon}_r + \dot{\epsilon}_\theta = 0 = \frac{\partial u}{\partial r_o} + \frac{u}{r_o} = 0 \qquad \text{(C-1)}$$

From Eq. (B-1) we know that,

$$u = \frac{mat_o}{r_o}$$

differentiating w.r.t. r_o we obtain

$$\dot{\epsilon}_r = \frac{\partial u}{\partial r_o} = - \frac{mat_o}{r_o^2}$$

and dividing by r_o we have

$$\dot{\epsilon}_\theta = \frac{u}{r_o} = \frac{mat_o}{r_o^2}$$

Integrating w.r.t. t we have

$$\epsilon_r = -\frac{mat_o t}{r_o^2} + C(r_o)$$

$$\epsilon_\theta = \frac{mat_o t}{r_o^2} + C'(r_o)$$

where $C(r_o)$ and $C'(r_o)$ are the constants of integration.

at $t = t_o$ we know from Eq. (B-5) that

$$\epsilon_r = -\frac{mat_o^2}{2r_o^2}$$

and

$$\epsilon_\theta = \frac{mat_o^2}{2r_o^2}$$

Substituting above we obtain

$$C = \frac{mat_o^2}{2r_o^2}$$

and

$$C' = -\frac{mat_o^2}{2r_o^2}$$

Hence,

$$\epsilon_r = -\frac{mat_o}{r_o^2}\left(t - \frac{t_o}{2}\right)$$

and

$$\epsilon_\theta = \frac{mat_o}{r_o^2}\left(t - \frac{t_o}{2}\right) \qquad \text{(C-2)}$$

Substituting in Eq. (10) we obtain

$$S_r = -\frac{E' mat_o}{r_o^2}\left(t - \frac{t_o}{2}\right)$$

and (C-3)

$$S_\theta = \frac{E' mat_o}{r_o^2}$$

The equilibrium equation is the same as Eq. (B-3) with $m = 0$, i.e., (constant velocity) that reduces to

$$\frac{\partial S}{\partial r_o} = 0 : \quad \text{or, } S = C_4(t)$$

where C_4 is the constant of integration. We evaluate C_4 from Eq. (B-4) which applies at $t = t_o$. Thus, $S = \rho ma\, \ell n\, (\frac{b}{r_o})$ which indicates that it is constant with respect to time.

The elastic solution during the constant velocity interval is found by substituting for S_r and S in the equations $\sigma_r = S + S_r$ and $\sigma_\theta = S + S_\theta$:

$$\sigma_r = \rho ma\, \ell n\, (\frac{b}{r_o}) - \frac{E' mat_o}{r_o^2}\left(t - \frac{t_o}{2}\right)$$

and (C-4)

$$\sigma_\theta = \rho ma\, \ell n\, (\frac{b}{r_o}) + \frac{E' mat_o}{r_o^2}\left(t - \frac{t_o}{2}\right)$$

When the material becomes plastic during the loading phase, the plastic flow will continue into the constant velocity phase. At $t = t_o$ the radius of the elastic-plastic interface R is given by combining Eqs. (10), and (B-2), substituting $r_o = R$, and then solving for R, when $S_r = K$. The radius of the elastic-plastic interface during the constant velocity period R_1, is found in similar fashion from Eqs. (10), and (C-2), for $S_r = -K$.

For $r_o < R$, the material is plastic, for $r_o > R_1$ the material is elastic. The stresses and strains in the plastic region are found as in the case of increasing velocity. Since we assume incompressibility during elastic and plastic cases the equation for velocity remains unaffected.

Hence,

$$u = \frac{mat_o}{r_o}$$

The stresses are given by $\sigma_r = S - K$ and $\sigma_\theta = S + K$ with $S_r^2 + S_r S_\theta + S_\theta^2 = K^2$ and $\sigma_r - \sigma_\theta = -2K$. Substituting into equilibrium equation (for $m = 0$) we obtain

$$\frac{\partial S}{\partial r_o} = \frac{2K}{r_o}$$

Integrating we obtain

$$S = 2K\ell n r_o + f(t)$$

At $r_o = R_1$ both the elastic and plastic solutions hold.

Thus,

$$\sigma_r = -K + S = 2K\ell n R_1 + f(t) - K$$

$$= \rho a \ell n\left(\frac{b}{R_1}\right) - \frac{E' mat_o}{2}\left(t - \frac{t_o}{2}\right)$$

Hence,

$$f(t) = \rho ma \ \ell n \left(\frac{b}{R_1}\right) - \frac{E' mat_o}{R_1^2} \left(t - \frac{t_o}{2}\right) - 2_k K \ \ell n \ R_1 + K$$

Therefore,

$$S = \rho ma \ \ell n \left(\frac{b}{R_1}\right) - \frac{E' mat_o}{R_1^2} \left(t - \frac{t_o}{2}\right) + 2K \ \ell n \frac{r_o}{R_1} + K \qquad \text{(C-5)}$$

Thus, the stresses for $r_o < R_1$ are given by

$$\sigma_r^p = \rho ma \ \ell n \left(\frac{b}{R_1}\right) - \frac{E' mat_o}{R_1^2} \left(t - \frac{t_o}{2}\right) + 2K \ \ell n \frac{r_o}{R_1}$$

and (C-6)

$$\sigma_\theta^p = \rho ma \ \ell n \left(\frac{b}{R_1}\right) - \frac{E' mat_o}{R_1^2} \left(t - \frac{t_o}{2}\right) + 2K \ \ell n \frac{r_o}{R_1} + 2K$$

The stresses for $r_o > R_1$ are given by Eq. (C-4).

where R_1 = elastic-plastic boundary during constant velocity phase.

APPENDIX D

SOLUTIONS DURING UNLOADING

In the final phase of the stress pulse the velocity decreases to zero, during $t_2 \leq t \leq t_3$ (see Fig. 1c). Let the deceleration constant be m'. The velocity during the unloading phase is given by

$$u = \frac{mat_o}{r_o} + \frac{m'at'}{r_o}, \text{ where } t' = t - t_2.$$

Differentiating w.r.t. r_o we obtain $\dot{\epsilon}_r = -\frac{a}{r_o^2}(mt_o + m't')$.

Integrating w.r.t. time t' we have

$$\epsilon_r = -\frac{a}{r_o^2}\left(mt_o t' + \frac{m'(t')^2}{2}\right) + C$$

at

$$t = t_2, \ \epsilon_r = -\frac{mat_o}{r_o^2}\left(t_2 - \frac{t_o}{2}\right)$$

Hence,

$$C = -\frac{mat_o}{r_o^2}\left(t_2 - \frac{t_o}{2}\right)$$

Therefore,

$$\epsilon_r = \frac{-a}{r_o^2}\left(mt_o t' + \frac{m'(t')^2}{2} + mt_o t_2 - \frac{mt_o^2}{2}\right)$$

and

$$\epsilon_r = -\frac{a}{r_o^2}F(t) \text{ and } \epsilon_\theta = \frac{a}{r_o^2}F(t) \qquad \text{(D-1)}$$

where

$$F(t) = mt_o t' + \frac{m'(t')^2}{2} + mt_o t_2 - \frac{mt_o^2}{2} \qquad \text{(D-2)}$$

Substituting in Eq. (10), we obtain

$$S_r = E' \epsilon_r = - E' \frac{a}{r_o^2} F(t) \qquad \text{(D-3)}$$

and

$$S_\theta = E' \epsilon_\theta = E' \frac{a}{r_o^2} F(t)$$

Substituting in the equilibrium equations we obtain from Eq. (B-3)

$$\frac{\partial S}{\partial r_o} = - \frac{\rho m' a}{r_o}$$

where m' is the deceleration rate.

$$S = \rho m' a \ell n \left(\frac{b}{r_o}\right) \qquad \text{(D-4)}$$

Thus, the elastic solution is given by

$$\sigma_r = S + S_r = - E' \frac{a}{r_o^2} F(t) + S$$

or

$$\sigma_r = \rho m' a \ell n \left(\frac{b}{r_o}\right) - E' \frac{a}{r_o^2} F(t)$$

and

$$\sigma_\theta = \rho m' a \ell n \left(\frac{b}{r_o}\right) + E' \frac{a}{r_o^2} F(t) \qquad \text{(D-5)}$$

for $t_2 \leq t \leq t_3$.

The plasticity condition, $S_r = -K$ and $S_\theta = K$ will continue into the unloading phase. Substituting in the equilibrium equation we obtain

$$\frac{\partial S}{\partial r_o} = \frac{2K}{r_o} - \frac{\rho m' a}{r_o}$$

After integration we have $S = (2K - \rho m' a)\, \ell n r_o + C_5$. Since at the radius of the elastic-plastic interface R', both the elastic and plastic solutions hold, we obtain

$$(2K - \rho m' a)\, \ell n R' + C_5 - K = \rho m' a\, \ell n \left(\frac{b}{R'}\right) - \frac{E' a}{(R')^2} F(t)$$

Hence,

$$C_5 = K - (2K - \rho m' a)\, \ell n R' + \rho m' a\, \ell n \left(\frac{b}{R'}\right) - \frac{E' a}{(R')^2} F(t)$$

Thus, for $r_o < R'$, the solution is given by

$$\sigma_r^p = (2K - \rho m' a)\, \ell n \frac{r_o}{R'} + \rho m' a\, \ell n \left(\frac{b}{R'}\right) - E' a F(t) \frac{1}{(R')^2}$$

and (D-6)

$$\sigma_\theta^p = (2K - \rho m' a)\, \ell n \frac{r_o}{R'} + \rho m' a\, \ell n \left(\frac{b}{R'}\right) - E' a F(t) \frac{1}{(R')^2} + 2K$$

or

$$\sigma_\theta = \sigma_r + 2K.$$

The value of R' is found from $S_r = -K = -\dfrac{E' a F(t)}{(R')^2}$

or

$$R' = \sqrt{\frac{E' aF(t)}{K}} \qquad \text{(D-7)}$$

The stresses for $r_o > R'$ are given by Eq. (D-5). At the end of the unloading phase, $t = t_3$, $mt_o = -m't'$, and $u = 0$.

APPENDIX E

AXIAL STRESSES

With plane strain conditions, we have $S_z = 0$. Using Eq. (7) we obtain $\sigma_z = S$. The final conditions given in Appendix D provide the following equation for S.

Elastic case $$\sigma_z = S = \rho m' a \ell n \left(\frac{b}{r_o}\right) \quad \text{(E-1)}$$

Plastic condition $$\sigma_z^p = S = \sigma_r^p + K \quad \text{(E-2)}$$

The axial stress for unloading with yielding is taken from Ref. 8

$$\Delta\sigma_z = \Delta\sigma_r - 2K \quad \text{(E-3)}$$

Thus, the final axial stress $(\sigma_z) = \sigma_z^p + \Delta\sigma_z$: or, combining Eqs. (E-2) and (E-3), we obtain

$$(\sigma_z)_F = (\sigma_r)_F - K \quad \text{(E-4)}$$

When the rivet is removed, $(\sigma_r)_F = 0$ at $r_o = a$.

Thus,

$$(\sigma_z)_F = -K \quad \text{(E-5)}$$

The axial stress for unloading without yielding is given by

$$\Delta\sigma_z = -(P - \sigma_r^p) \frac{a^2}{b^2 - a^2}$$

or, using Eq. (27), we have

$$\Delta\sigma_z = \Delta\sigma_r \frac{r_o^2}{r_o^2 - b^2}$$

and

$$(\sigma_z)_F = \sigma_z^p + \Delta\sigma_z = \sigma_r^p + K + \Delta\sigma_r \left(\frac{r_o^2}{r_o^2 - b^2}\right) \qquad \text{(E-6)}$$

Separate calculations are necessary to obtain axial stress distributions, since they are not included in the computer program discussed earlier.

Unclassified

SECURITY CLASSIFICATION OF THIS PAGE (When Data Entered)

REPORT DOCUMENTATION PAGE		READ INSTRUCTIONS BEFORE COMPLETING FORM
1. REPORT NUMBER RE-552	2. GOVT ACCESSION NO.	3. RECIPIENT'S CATALOG NUMBER
4. TITLE (and Subtitle) Advantages of Residual Stresses in Dynamically Riveted Joints		5. TYPE OF REPORT & PERIOD COVERED Research Report 6. PERFORMING ORG. REPORT NUMBER
7. AUTHOR(s) Basil P. Leftheris		8. CONTRACT OR GRANT NUMBER(s)
9. PERFORMING ORGANIZATION NAME AND ADDRESS Grumman Aerospace Corporation Research Department Bethpage, New York 11714		10. PROGRAM ELEMENT, PROJECT, TASK AREA & WORK UNIT NUMBERS
11. CONTROLLING OFFICE NAME AND ADDRESS		12. REPORT DATE February 1978 13. NUMBER OF PAGES 77
14. MONITORING AGENCY NAME & ADDRESS(if different from Controlling Office)		15. SECURITY CLASS. (of this report) 15a. DECLASSIFICATION/DOWNGRADING SCHEDULE

16. DISTRIBUTION STATEMENT (of this Report)

Approved for public release, distribution unlimited

17. DISTRIBUTION STATEMENT (of the abstract entered in Block 20, if different from Report)

18. SUPPLEMENTARY NOTES

19. KEY WORDS (Continue on reverse side if necessary and identify by block number)

Residual stresses, interference fasteners

20. ABSTRACT (Continue on reverse side if necessary and identify by block number)

This report presents an analytical method for calculating residual stresses in joints riveted dynamically, results of the Moire' experimental method for measuring the residual strain distribution around a rivet hole, and describes an experimental method for measuring the radial velocity of an expanding rivet. The advantages of compressive residual stresses in dynamically riveted joints are demonstrated through constant amplitude fatigue testing.

The particular cases in which residual stresses were investigated include aluminum 7075-T6 and 2024-T3 sheet with ¼ in. diameter holes, riveted with

DD FORM 1 JAN 73 1473 EDITION OF 1 NOV 65 IS OBSOLETE
S/N 0102-014-6601

unclassified

SECURITY CLASSIFICATION OF THIS PAGE (When Data Entered)

20. A-286 rivets installed with the Stress wave riveting expands the rivet radially under high acceleration to achieve favorable stress distributions. Analytical predictions of these stress distributions are compared with experimental results obtained using the Moire' photoelastic method. To demonstrate the benefits of compressive residual stresses in rivet joints, fatigue specimens made of 2024-T81 aluminum were used. The specimens were tested at constant amplitude load cycling. In the first series of tests, the fatigue lige of specimens with residual stresses was approximately ten times higher than the fatigue life of specimens with open holes. In the second series, precracked specimens with a 0.05 in. crack in each hole were riveted with the StressWave Riveter. The cracks were oriented so that the fatigue loading was normal to the crack path. The fatigue life of these specimens was also approximately ten times higher than the fatigue life of those specimens with precracked holes with rivets.